FRACTURE TOUGHNESS MEASUREMENTS IN A HSLA STEEL BY J INTEGRAL METHOD

by

G. BABU VISWANATHAN

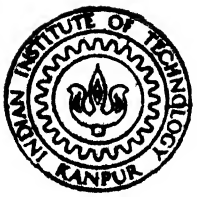

DEPARTMENT OF METALLURGICAL ENGINEERING
INDIAN INSTITUTE OF TECHNOLOGY KANPUR

AUGUST, 1985

FRACTURE TOUGHNESS MEASUREMENTS IN A HSLA STEEL BY J INTEGRAL METHOD

A Thesis Submitted
In Partial Fulfilment of the Requirements
for the Degree of

MASTER OF TECHNOLOGY

by
G. BABU VISWANATHAN

to the

DEPARTMENT OF METALLURGICAL ENGINEERING
INDIAN INSTITUTE OF TECHNOLOGY KANPUR
AUGUST, 1985

ME - 1985 - M - VIS - FRA

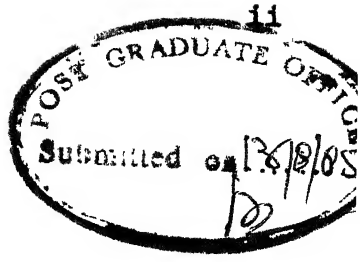

CERTIFICATE

This is to certify that this work entitled 'Fracture Toughness Measurements in a HSLA Steel by the J-Integral Method' has been carried out under our supervision and has not been submitted elsewhere for a degree.

Dr. Prashant Kumar
Assistant Professor
Department of Mechanical Engineering
Indian Institute of Technology
Kanpur

Dr. M.N. Shetty
Professor
Department of Metallurgical Engineering
Indian Institute of Technology
Kanpur

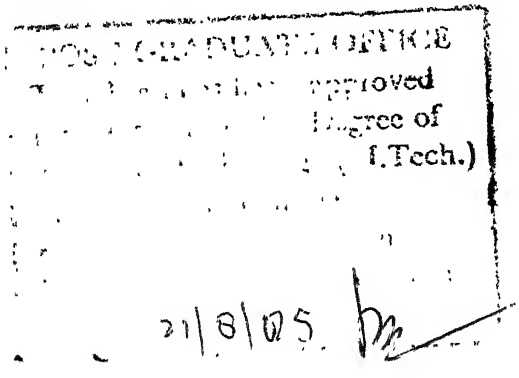

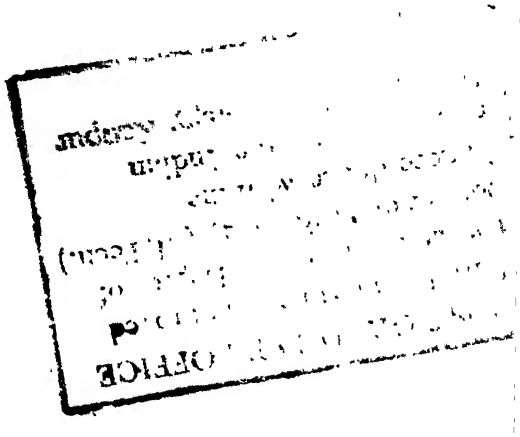

ACKNOWLEDGEMENTS

I express my deep sense of gratitude to Dr. M.N. Shetty and Dr. Prashant Kumar for their valuable guidance. I highly appreciate their understanding, keen encouragement, kind help extended to me in carrying out the project.

I am very thankful to Mr. V.P. Gupta for being extremely helpful throughout my work and for his excellent sketches in this thesis.

Thanks are due to Mr. B.K. Jain for his utmost co-operation in carrying out my experiments and Mr. R.N. Srivastava for his excellent typing work.

It is impossible to fully appreciate in words the warmth and affection that my inumerable friends accorded to me throughout the period of my stay here.

I personally thank all the people who have been associated with me in all dimensions and in all spaces.

- Gopal Babu Viswanathan

CONTENTS

LIST OF FIGURES

ABSTRACT

Fracture studies are conducted in a high strength low alloy steel. The concept of J-integral in elasto-plastic fracture mechanics, is used to determine the fracture criterion. Slow three point bend tests are carried out in machined and notched specimens and the value of J is calculated from the area under load-displacement curve obtained in the test. The bend tests are carried out over a range of temperatures from -170°C to 340°C and the dependence of J values on temperature has been shown as J vs. temperature plot. Exhibiting a plateau region, J decreases sharply as we approach liquid nitrogen temperature, with a ductile to brittle transition temperature of about -35°C.

Direct tensile tests and Charpy impact tests are also carried out over the same range of temperatures, to correlate J with other mechanical properties. The plateau region observed in the J vs. temperature plot has been found to correspond well with the region of 'dynamic strain ageing' that occurs over the same temperature range in direct tensile tests. The Charpy impact test show a ductile to brittle transition for same steel to about 55°C and this shift in the transition temperature from -35°C to 55°C between J vs. temperature plot and impact energy vs. temperature plot is attributed to strain rate effects.

CHAPTER I

INTRODUCTION

1.1 GENERAL

For the prevention of failure in structures, engineers have traditionally looked for quantitative criteria permitting prediction of the entire structure's behaviour from simple laboratory tests on small specimens. A brittle fracture is characterised by rapid propagation of flows occurring at stresses well below the yield stress and involving very little plastic deformation. For this case, suitable tests were conducted which had long been exclusively based on the use of notched bar specimens subject to impact loading at various temperatures, preferably covering the entire range of possible service temperatures. The single-parameter criterion thus obtained is the so called 'transition temperature', marking a change between relatively low and high energy absorption by the specimens in fracture. This method does not always give clear-cut transition temperature and in addition, this criterion ignores the influence of flow size, shape and of the stresses in the structure. Griffith formulated a theory as early as 1920, which stated that an existing crack would propagate if the total energy of the system would thereby be lowered. This research led to the proof by Irwin, in 1957, that this energy approach is equivalent to stress-intensity approach

according to which fracture occurs if the stresses near the crack tip reach a critical value, characteristic of the material.

This, Griffith-Irwin concept was subsequently expanded into the field of fracture mechanics. The validity of this approach was predicted upon the assumption of linear elastic behaviour of the material surrounding the crack tip. This linear elastic fracture mechanics (LEFM) approach provides quantitative expressions for the fracture stress in terms of crack size and shape and loading conditions.

For more common structural and pressure vessel steels serving at and above room temperature this condition becomes unrealistic for the actual structure and difficult to achieve in test specimens, due to the spread of plastic behaviour around the crack tip. For the same reason extensive work has been undertaken to extend the single-parameter fracture mechanics approach into the realm of elasto-plastic material behaviour. The result of this is the discovery of the main concepts crack opening displacement (COD) and J-integral which give one-parameter criteria that have reached the stage of practical application.

Both concepts suited our aim to find out the fracture criterion over a range of temperatures from sub-zero level to high temperature level we opted for the J-integral technique, since the method is simpler to carry out and the interpretation of the results are exact without much error. This method suited especially for high

temperatures. We cho bend type specimens and conducted slow bend tests to determine the J-values. The method used in our study popularly known as J-estimation procedure is simple and accurate. We have also established the reasons for the behaviour of J dependence of temperature, with the material behaviour. The HSLA steel in our study exhibit dynamic strain ageing over the temperature range 150°C-230°C. This behaviour is clearly reflected in the J versus temperature plot, which results in a plateau region over this same temperature range. The temperature dependence of J has then been correlated to the properties in direct tensile tests and charpy impact tests. This kind of work has been done for the first time in this area. It is very essential for scientists and engineers to know the material behaviour, which has direct impact on the fracture properties of the material.

1.2 LINEAR ELASTIC FRACTURE MECHANICS

1.2.1 Energy balance approach to fracture

The energy balance approach to the study of the fracture phenomenon in cracked bodies was originally proposed by Griffith [1]. He proposed that a brittle material contains a population of fine cracks which produces stress concentrations of sufficient magnitude so that the theoretical cohesive strength is reached in localized regions at a nominal applied stress which is well below the critical theoretical value. Griffith established the following criterion for the propagation of a crack. 'A crack will propagate when the decrease in elastic strain energy is at least equal to the energy required to create the new crack surface'. From the practical viewpoint the demonstration that a functional relationship exists between failure stress and crack length was a significant step forward.

Almost thirty years after Griffith's contribution, Irwin and Orwan [2] suggested a modification to the original formulation so that limited plastic deformationprior to failure could be included.

Griffith's equation is $$\sigma = \left(\frac{2E\,\gamma_s}{\pi c}\right)^{1/2} \qquad (1)$$

where σ is the stress required to propagate a crack in a brittle material, E is the Young's modulus, γ_s is the surface energy and c is the crack size.

Orwan [3] suggested that Griffith's equation would be made more suitable with brittle fracture in metals by the inclusion of a term $_p$ expressing the plastic work required to extend the crack

$$\sigma_f = \frac{\sqrt{2E(\gamma_s + \gamma_p)^{1/2}}}{\pi c} \approx \frac{\sqrt{E\gamma_p}}{c} \qquad (2)$$

The surface energy term can be neglected.

Orowan pointed out that the approach would be valid only if plastic deformation was confined to thin layers adjacent to the crack walls. He demonstrated that fracture stress was inversely proportional to the square root of crack length by the modified theory. However, the value of γ_p calculated from these results was 3 to 5 times that to be expected from the X-ray analysis of the fractured surfaces. He concluded that these results would be better explained using a crack tip characterizing parameter approach.

On the other hand Irwin suggested that if the fracture process was essentially similar for different loadings and geometries, the fracture event would occur when the strain energy release rate reached a critical value. This critical value could be regarded as a material property to be determined for a fracture test. Irwin and Kies [4] noted that the strain energy in an elastic body could be represented by the relationship

$$U = \frac{Q^2 c}{2} \qquad (3)$$

where Q is the characterizing force and C the compliance of the body, i.e. the displacement at the point of application of Q.

From this expression it immediately follows that the strain energy release rate, with respect to crack extension is given by

$$\frac{\partial U}{\partial a} \equiv \frac{1}{2} Q^2 \frac{\partial C}{\partial a} \qquad (4)$$

By measuring the compliance of a test specimen, or a component model, with various crack lengths the value of $\partial c/\partial a$ as a function of crack length could be obtained. A fracture test could be interpreted by evaluating $\partial U/\partial a$ at fracture using the fracture load and the value of $\partial c/\partial a$ for the appropriate crack length.

Irwin [5] proposed an alternative interpretation of critical strain energy release rate when he suggested that this quantity could be regarded as a force. In these terms, fracture was described as a rate controlled process driven by this force, which was defined as the irreversible energy loss per unit area of newly created surface. This force, denoted as G (after Griffith) would have a critical value, G_c when a crack starts to propagate.

In situations where fracture is preceded by limited plastic deformation there is strict equivalence between the strain energy release rate concept G, and the stress intensity approach which will be discussed in the next section. Thus the techniques available for determining stress intensity

factors are equally valid for determining G. However, in situations where extensive plastic deformation takes place prior to failure the relationship between an energy balance approach and a crack tip environment approach becomes more tenuous. Therefore one has to be careful when interpreting fracture behaviour in these situations.

1.2.2 Stress intensity factor approach to fracture

The previous section discussed about the development of fracture mechanics on the basis of an energy balance approach. The fracture phenomena which focuses attention on the mechanical environment near the tip of a crack was developed by Irwin and is generally known as the stress intensity factor approach.

a) Fracture modes

In dealing with the stress intensity factor there are several modes of deformation that could be applied to the crack. These have been standardized and shown in Figure 1. Mode I, the crack-opening mode, refers to a tensile stress applied in y direction normal to the faces of the crack. This is the usual mode for fracture toughness tests and a critical value of stress intensity determined for this mode would be designated as K_{Ic}. In engineering practice the importance of the opening mode I far exceeds that of the other modes. This work is limited to mode I unless specifically stated otherwise.

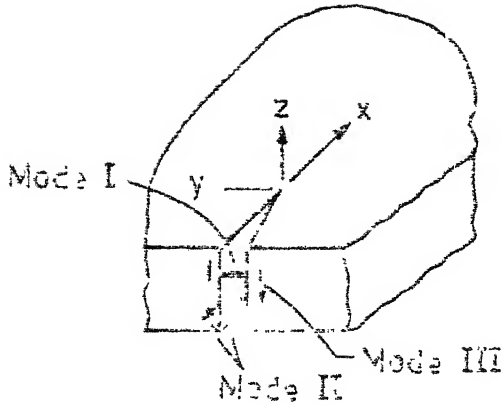

Fig. 1. Crack-deformation modes.

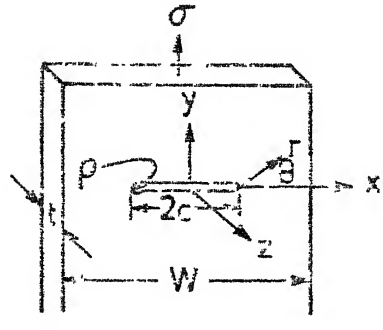

Fig. 2. Model for equations for stresses at a point near a crack.

Irwin [6] laid the foundation for the important area of fracture mechanics. He proposed that fracture occurs at a fracture stress corresponding to a critical value of the crack-extension force, where equation 1 is rewritten as

$$\sigma_f = \left(\frac{EG}{\pi c}\right)^{1/2} \tag{5}$$

$$G = \pi c \frac{\sigma^2}{E} \tag{6}$$

G may also be considered the strain energy release rate i.e. the rate of loss of energy from the elastic stress field to the inelastic process of crack extension. In the early stages this value of G established through a standard method served the purpose of measuring a fracture criterion.

b) The elastic crack tip stress field

Using Westergaard's [7] complex stress functions, Irwin [8] demonstrated that the elastic stress field near the tip of the crack in an infinite sheet could be described for mode I.

The stress distribution at the crack tip in a thin plate for an elastic solid in terms of the coordinates shown in Figure 2 is given by the following equations:

$$\sigma_x = \sigma\left(\frac{c}{2r}\right)^{1/2} \left[\cos\frac{\theta}{2}\left(1 - \sin\frac{\theta}{2}\sin\frac{3\theta}{2}\right)\right] \tag{7(a)}$$

$$\sigma_y = \sigma\left(\frac{c}{2r}\right)^{1/2} \left[\cos\frac{\theta}{2}\left(1 + \sin\frac{\theta}{2}\sin\frac{3\theta}{2}\right)\right] \tag{7(b)}$$

$$\tau_{xy} = \sigma\left(\frac{c}{2r}\right)^{1/2} \left[\sin\frac{\theta}{2}\cos\frac{\theta}{2}\cos\frac{3\theta}{2}\right] \tag{7(c)}$$

(7)

where σ = gross nominal stress = $\frac{P}{wt}$ and these equations are valid for $c > r > P$.

Irwin pointed out that the above equations indicate that the local stresses near a crack depend on the product of the nominal stress σ and the square root of the half-flaw length. He called this relationship the stress-intensity factor K, where for a sharp elastic crack than infinitely wide plate, K is defined as

$$K = \sigma \sqrt{\pi c}$$

K has the unusual dimensions of $MN/m^{3/2}$ or MPa $\sqrt{mm}$. Using these definitions for K, the equations for the stress field at the end of a crack can be written

$$\sigma_x = \frac{K}{\sqrt{2\pi r}} \left[\cos \frac{\theta}{2} \left(1 - \sin \frac{\theta}{2} \sin \frac{3\theta}{2}\right)\right] \qquad 8(a)$$

$$\sigma_y = \frac{K}{\sqrt{2\pi r}} \left[\cos \frac{\theta}{2} \left(1 + \sin \frac{\theta}{2} \sin \frac{3\theta}{2}\right)\right] \qquad 8(b)$$

$$\tau_{xy} = \frac{K}{\sqrt{2\pi r}} \left[\sin \frac{\theta}{2} \cos \frac{\theta}{2} \cos \frac{3\theta}{2}\right] \qquad 8(c)$$

(8)

Values of K for many geometrical cracks and many types of loading may be calculated from the theory of elasticity. From the above discussion one can easily establish the relationship between 'G' the crack extension force and the stress intensity factor 'K'

$$G = \frac{1 + k}{8\mu} K^2 \qquad (9)$$

where μ is the shear modulus and

k is a function of Poisson's ratio (ν)

viz. $K = 3 - 4\nu$ for conditions of plane strain

$= \frac{3 - \nu}{1 + \nu}$ for conditions of plane stress.

The above relationships show that the attainment of a critical extension force is equivalent to a critical stress environment. Fracture in this situation can be characterized by the attainment of a critical value of K.

Elastic analysis has shown that the stress environment around a crack tip was entirely similar to all situations to within a linear scaling factor. By means of tests on suitably shaped and loaded specimens it was possible to determine the material property K_{Ic} (or G_{Ic}) by defining it as the value of K_1 (or G_1) operative at the point of fracture. The value of K_1 at the point of fracture was found to be strongly dependent on plate thickness. Only after a certain thickness is exceeded critical value will be regarded as a material property. K_{Ic}, dependent only on the testing environment. The variation in the apparent value of K_{Ic} has been attributed to the through the thickness change in constraint along the crack front. The plastic regions that are near a free surface are practically in a condition of plane stress whilst those remote from such a surface approach conditions of plane strain. When thickness is sufficient the fracture behaviour will be dominated by the region of constrained plastic deformation, a

characteristic flat fracture will occur and conditions are described as 'plane strain'.

So far the basic philosophy of the stress intensity approach has been discussed without mentioning precisely how specific cases are dealt with. Obviously to interpret test results or to make design calculations, it is necessary to have explicit expressions for K_I for specific geometries and loading conditions. The determination of stress intensity factors is a specialist's task necessitating the use of a number of analytical and numerical techniques. It would be appropriate to discuss these in a separate chapter. The important point is that it is always possible to determine K_I to a sufficient accuracy for any given geometry or set of loading conditions.

In general stress intensity factors may be written in the form

$$K_I = \sigma\sqrt{a}\, Y\left(\frac{a}{W}\right) \qquad (10)$$

where σ is a characterizing stress

a is a characterizing crack length

W is a characterizing dimension

and $Y(\frac{a}{W})$ is a calibration function which defines K_I for the specific body under consideration.

Figure 3 shows three configurations with the corresponding values of $Y(\frac{a}{W})$. Thus for example a fracture test on a three-point bend specimen would be interpreted by substituting the appropriate value of a/W in the polynomial

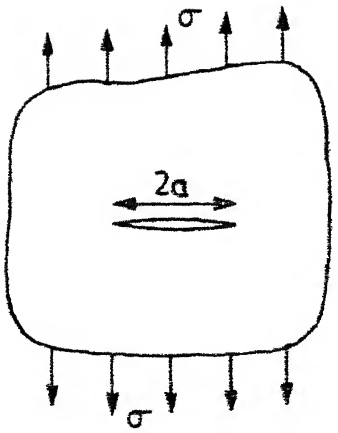

$$Y\left(\frac{a}{W}\right) = \sqrt{\pi}$$

(a) Isolated crack in an infinite plate

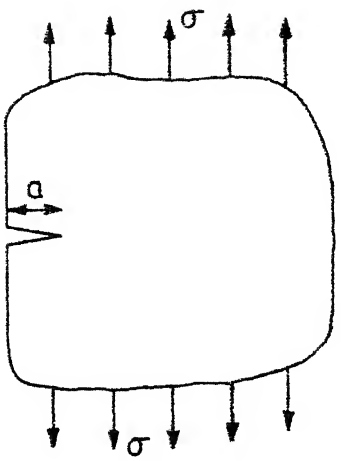

$$Y\left(\frac{a}{W}\right) = 1.12\sqrt{\pi}$$

(b) Surface crack in a semi-infinite plate

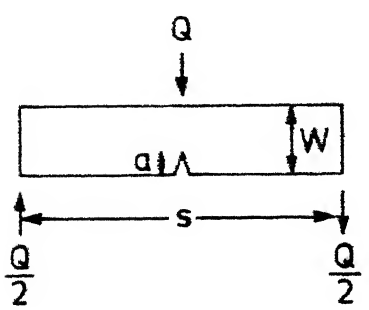

$$\sigma = \frac{6M}{tW2} \quad M = \frac{QS}{4}$$

t = Plate thickness

$$Y\left(\frac{a}{W}\right) = 1.93 - 3.07\left(\frac{a}{W}\right) + 14.53\left(\frac{a}{W}\right)^2 - 25.11\left(\frac{a}{W}\right)^3 + 25.8\left(\frac{a}{W}\right)^4$$

(c) Surface crack in three-point bend specimen

Fig. 3. Some crack configurations.

for $Y(\frac{a}{W})$. Figure (c) noting the load at fracture and thus determining the value of K_I at fracture. Alternatively, if it is necessary to estimate the maximum permissible depth of a surface defect in a thick component subject to uniform stress, use is made of the solution given in Figure 3(b). Here the stress intensity factor is given by

$$K_I = 1.12 \sigma \sqrt{(\pi a)}$$

Consequently a knowledge of a critical value of K_I as determined by an appropriate fracture test, and the applied stress level permits the critical value of crack depth to be determined.

To summarize, the fracture event is interpreted as being characterized by the attainment of a critical value of the stress intensity factor, K_{Ic}. Geometry and loading conditions influence this environment through the parameter K_I, which may be determined by suitable analysis. A knowledge of K_{Ic}, obtained from a suitable test, thus provides a means of predicting the fracture behaviour in real structures. The sensitivity of structures to other phenomena such as fatigue crack growth and stress corrosion cracking can likewise be predicted on the basis of suitably performed tests interpreted in terms of the stress intensity approach.

1.3 YIELDING FRACTURE MECHANICS

The prime objective of yielding fracture mechanics is to describe the fracture circumstances for a material of

considerable ductility in the presence of a defect. As with other branches of fracture mechanics, a means is sought whereby fracture observed in the laboratory can be interpreted in terms of a material property, toughness. Just as in linear elastic fracture mechanics (LEFM) one approach is to characterize the singular stress, strain and displacement fields around the tip of a sharp crack by a single parameter so too in yielding fracture mechanics efforts have been made to find one parameter characterization of the elastic-plastic stress and strain fields local to the crack tip. It is argued, as in LEFM, that if such a parameter can be found, then for a given composition, temperature, strain rate and environment a process such as fracture supposed to be governed by circumstances at the crack tip, must occur when this parameter reaches a critical value.

1.3.1 The role of extent of plasticity

The notion of plastic constraint and associated terms such as small scale or contained yield and constrained or unconstrained yielding into proper perspective, the different ways in which a cracked component may fail when loaded beyond the range to which LEFM is applicable will now be surveyed briefly. A centre-cracked panel loaded in tension is taken as a simple example.

A stress very near to the crack tip(not specifically defined here but taken as representative of the local stress conditions) is denoted by L^{σ} the uniaxial yield stress

by σ_y, net section stress by σ_n and the uniform stress remote from the crack by σ. It is useful to distinguish four regimes, which can loosely be described as follows.

(a) $L^{\sigma} > \sigma_y > \sigma_n > \sigma$: Yielding limited to a zone in the immediate vicinity of the crack, to a very small extent. This is the LEFM problem. If failure occurs it is usually by unstable, rapid propagation of the crack.

(b) $L^{\sigma} > \sigma_y > \sigma_n > \sigma$: Yielding is extensive but does not spread to a lateral boundary of the structure and thus contained. This is a regime that can be called elastic-plastic and to which yielding fracture mechanics can be applied. Failure usually occurs by unstable rapid propagation of the crack.

(c) $L^{\sigma} > \sigma_n > \sigma_y > \sigma$: Yielding is very extensive and spreads to the lateral boundary ahead of tne crack, and thus uncontained. This is the regime that can be called gross yield, to which yielding fracture mechanics must be applied. For configurations with little lateral constraints and low hardening, tough materials may fail by plastic collapse of the net section, whilst for less though materials a crack may spread by stable or unstable growth.

(d) $L^{\sigma} > \sigma_n > \sigma > \sigma_y$: Since the applied stress σ is greater than the yield stress, extensive plasticity occurs along the components as well as the cross section implying work hardening of the net section.

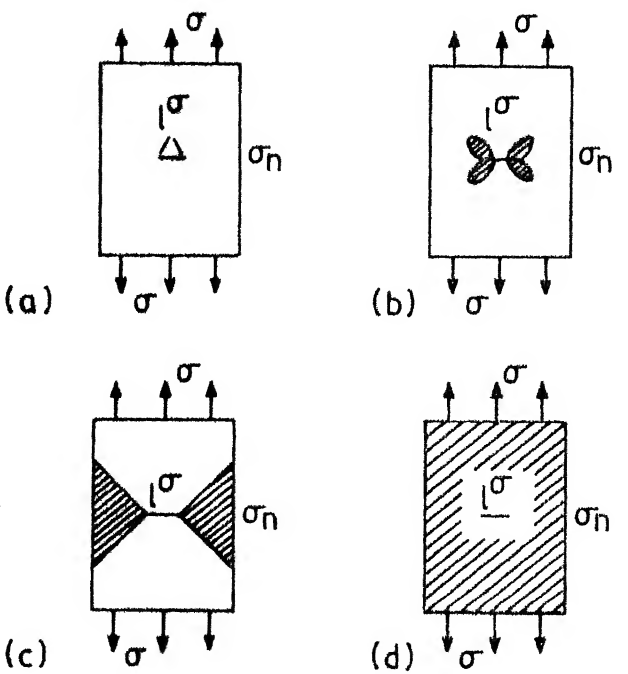

Fig. 4. Schematic representation of increasing degrees of yielding

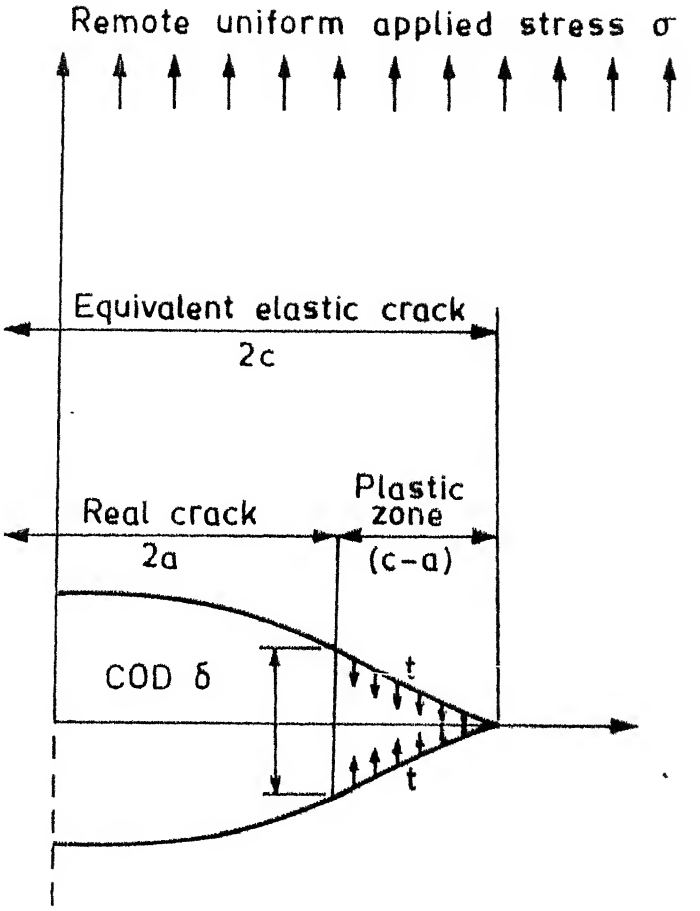

Fig. 5. The Dugdale model for crack tip plasticity

This is the regime that can be called general yield. Crack propagation in this case may still be the failure mode.

These four conditions are shown schematically in Figure 4. It must be clear that the stress levels used to describe the four states merge from one condition to the other and are affected by configuration, induced biaxial and triaxial stresses and work hardening. Clearly, the regimes starting in (b) and extending through (c) and for some materials into (d) are those that constitute the realm of yielding fracture mechanics of interest here.

1.3.2 Concept of crack opening displacement (COD)

The method is based on the assumption - put forward independently by Wells [9], Cottrell [10] and Bavenblatt [11] - that where significant plasticity occurs the fracture process will be controlled primarily by the intense deformations adjacent to the crack tip, and that the separation of the crack faces, or crack opening displacement will be a measure of the intense deformation. Crack extension will then begin at some critical value of this crack opening displacement, according to the particular micromode of fracture that occurs. Hence the method requires analytical prediction of displacements near the crack tip.

The model, proposed by Dugdale [12] and Barenblatt [11] considers an infinite plate with a central crack, length 2a, subjected to a remotely applied uniform stress .

The plasticity at the tip of the crack is represented by a notional increase in the crack length to some value, 2c with the faces of the 'crack' over the distances (c-a) from both ends partly restricted from opening by a restraining stress, 't' acting directly on the crack faces. Later Wells [13] noticed that in practice the tip of a slot subjected to plastic deformation opened with a near square ended contour, giving a definite tip opening - the crack opening displacement - (COD) as in Figure 5. He proposed that the COD, δ, was a measure of crack tip deformation and that fracture might occur when a critical value of this parameter, δ_c, was reached. This proposal was pursued experimentally and theoretically by many scientists who have showed that it was broadly consistent with fracture results from large tension and bending tests.

In early applications of this model, t was equated to the uniaxial yield stress, σ_y and relationships obtained for the length, 2c, to which the notional plastic zone extended in terms of the real length, 2a, and the applied stress σ

$$\frac{a}{c} = \cos \frac{\sigma\pi}{2\sigma_y} \qquad 11$$

The COD, δ, at the tip of the real crack was then evaluated as

$$\delta = \frac{8\sigma_y a}{\pi E} \log \sec \frac{\pi\sigma}{2\sigma_y} \qquad 12$$

By expanding the secant term it was found that

$$\delta = \frac{\pi \sigma^2 a}{E \sigma_y} \left[1 + \frac{\pi^2}{24} \left(\frac{\sigma}{\sigma_y}\right)^2 + \ldots\right] \qquad 13$$

However renumbering the definition of strain-energy release rate in LEFM, for the infinite plate with centre crack 2a

$$G = \frac{K^2}{E} = \frac{\pi \sigma^2 a}{E} \qquad 14$$

It is at once seen that the first term in equation 13 corresponds to

$$G = \sigma_y \delta \qquad 15$$

If the plastic zone correction factor for plane stress is used then the modified LEFM expression is

$$G = \frac{\pi \sigma^2 a}{E} \left[1 + \frac{1}{2} \left(\frac{\sigma}{\sigma_y}\right)^2\right] \qquad 16$$

which together with equation 15 differs from the equation 13 by a fairly small amount in the coefficient of the second term. The relationship $G = t\delta$ is consistent with the work done to close an element of crack, from the reasoning of mechanics on either the macro or dislocation level, so that this model used with the restraining stress $t = \sigma_y$ appears to be a logical extension to LEFM for plane stress.

Turning to the weaknesses in the model, the most obvious of these is the representation of plastic yielding by an elastic material with only a line of plasticity ahead of the crack. This is not unreasonable for plane stress, but unrepresentative for plane strain. For reasons that are not wholly apparent, the usage of the Dugdale model has

retained the plane stress assumption of $t = \sigma_y$. It has in fact suggested that this inconsistency might be avoided through the use of a constrained yield stress

$$t = m \cdot \sigma_y \qquad (17)$$

where m might be $\sqrt{3}$ (from plastic zone correction) or even as high as 3 for yielding material analysed for contained yielding.

Still by using these modified expressions for finding the fracture criteria there exists some discrepancies between theory and experiment. Thus the above model ignores the effect of a finite plate and of a work hardening material.

1.3.3 Concept of J-integral

Of the many parameters proposed to correlate elastic-plastic fracture behaviour, the J-integral as proposed by Rice [14] has been one of the most promising. The J-integral was used originally as an analytical tool for crack-tip stress and strain determination. It was first proposed as a fracture parameter, labelled J_{Ic}, with supporting experimental method proposed was fairly cumbersome. Easier experimental methods for determining J_{Ic} have been developed. A considerable amount of new work has been conducted both in supporting the use of J_{Ic} as an elastic-plastic fracture criterion and in developing the testing techniques for determining J_{Ic}.

a) J-theory in general

The J-integral as proposed by Rice [14] is a two dimensional energy line integral (ref. Figure 6):

$$J = \int W\, dy - X \frac{\partial u}{\partial x}\, ds$$

where W is the strain energy density

$$W = \int_{o}^{\varepsilon_{mn}} \sigma_{ij}\, d\, \varepsilon_{ij} \qquad (19)$$

is the traction vector defined by the normal n along the path of integration, , $T_i = \sigma_{ij} n_j$, u is the displacement vector, and S is a length along . The J-integral is path independent and is applicable to elastic material or elastic-plastic material when treated by a deformation theory of plasticity.

The J-integral characterizes the crack tip field the basis of which is provided by the works of Hutchinson [15] and Rice and Rosengren [16]. They have extended fracture mechanics concepts to cases of large scale yielding which also assumes the crack tip singularity. They indicate that the product of plastic stress and strain approaches a $\frac{1}{r}$ singularity; r being a near tip crack field length parameter. The crack tip singularity is uniquely dependent on the material constitutive relations. For a deformation theory of plasticity McClintock [17] has demonstrated, through the crack tip plastic stress and strain equations expressed from the Hutchinson, Rice, Rosengren (HRR)

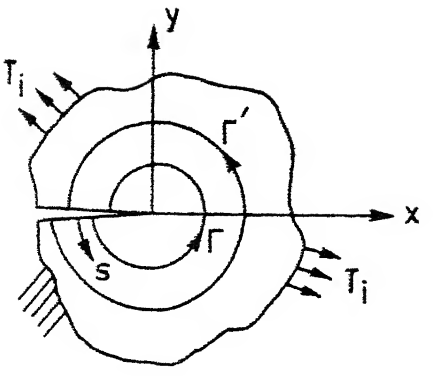

Fig. 6. Arbitrary contour over which J integral is evaluated.

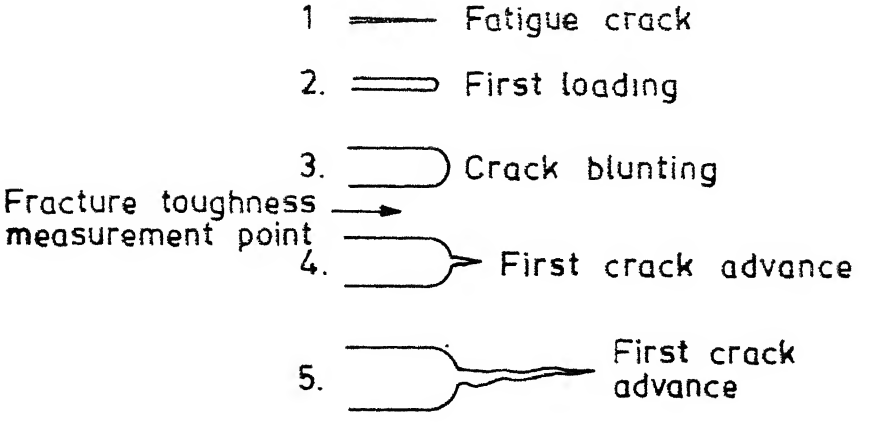

Fig. 7. Crack-tip schematic of the fracture process.

singularity, the existence of singularity in r whose strength is the J-integral.

The J-integral has another important advantage as a fracture criterion. Broberg [18] considered growth criteria for a nonlinear elastic body containing a crack. For such a body, stress and strain singularities occur at the crack tip. This region ahead of the crack tip is termed as the end region outside which the material may be regarded as a continuum. As the load is increased, the end region eventually reaches a critical state at which the crack starts moving. One prominent feature of the end region at critical state is that the state is neither dependent on the distribution of loads nor on the crack length. It simply and solely depends on the material itself. The end region or plastic zone can be specified by J_c, as it reaches the critical state.

From the foregoing discussion, it is evident that J-integral displays three prominent features attractive to its use as a fracture criterion namely,

(i) J-integral as a field parameter indicates the stress and strain distribution in a cracked body.

(ii) It describes the crack tip region by specifying the strength of the singularity.

(iii) Critical value of J-integral, J_c is a material property which can be used as a fracture criterion.

The J-integral can be conveniently evaluated experimentally through its energy rate interpretation as follows.

It may be noted that in equation (5) the two terms in the integral namely W and $T_i \frac{\partial u_i}{\partial x_i}$, have the dimensions of energy. Thus, J is an energy related quantity. In fact, Rice [14] has shown that the J-integral is equal to the change in potential energy for a virtual crack extension

$$J = -\frac{du}{da} \qquad (20)$$

where u is the potential energy per unit thickness

a is the crack length.

Equation (20) expresses an energy process where J is identical to G, the crack driving force. For the case of plastic behaviour where deformation is not reversible, J loses its significance as a crack driving force. It can be considered as an energy comparison between two similar bodies identically loaded which have incrementally differing crack sizes. The line integral definition of J in Equation (18) is most useful for an analytical determination of J where numerical methods are employed. The energy rate interpretation is used for experimentally determining J. Equation (19) represents an exact method for experimentally measuring J; however, for most testing purposes, an approximation to Equation (3) is used.

b) Limitations of J_{IC} approach

(i) Since the Rice energy line integral is expressed only in two dimensions, the J approach is therefore, limited to problems of plane strain or generalised plane stress.

(ii) Another limitation is that since J is shown to be path independent for deformation plasticity theory, the use of J as a fracture criterion should be compatible with the assumptions of deformation plasticity. This would restrict its use to monotonic loading and zero crack extension since any unloading cannot be treated by this theory of plasticity. Any crack extension necessarily implies unloading near the crack tip. In general, structures failing in plane stress exhibit some subcritical crack growth. Hence, the J integral failure criterion may be limited to the case of plane strain which is implied by the subscript I in J_{Ic}.

(iii) Also, since J is taken as the single parameter which characterizes the strength of the crack tip singular field equations, the size of the test specimen must be sufficient so that the crack-tip field equations are undisturbed by the specimen boundaries.

c) J as a fracture criterion

The fracture process starts with a sharp crack when the specimen or structure containing that crack is unloaded. For a test specimen the crack is introduced by fatiguing at a low ΔK level before the fracture test is conducted. As the crack undergoes loading the crack tip becomes blunted. This blunting increases with an increase in loading until a load is reached where a crack advance occurs ahead of the original blunted crack (ref. Figure 7). At the point where the first crack advance occurs the fracture toughness measurement point is defined. In terms of J this point is labelled J_{Ic}.

This model tray not strictly characterize the actual physical process. Cracking may begin ahead of the original blunted crack as voids are opened and joined. However, this model gives a general description of the fracture process which can then be related to a fracture parameter such as J. A physical application of the model is conceived more easily when cracking occurs in a ductile tearing mode.

1.4 METHODS FOR FRACTURE TOUGHNESS MEASUREMENT

Standard test method for the determination of K_{Ic} has been approved by ASTM Ref. Standard Test Method for

Plane Strain Fracture Toughness of Metallic Materials - ASTM Designation E399-74. The ASTM procedures have been divized so as to permit measurement of K_{Ic} and displacement (COD) under identical conditions with the same laboratory equipment and in the same test.

The unified testing procedure is

1. A machined notched test piece is used in which a tensile stress is developed at the notch tip either by tension or by bending.
2. The test piece is subjected to fatigue loading to start a sharp crack and develop it to the desired length.
3. The test piece is then loaded in tension or bending and a record is taken of the load against the opening displacement of the two sides of the notch. The test is continued until fracture occurs.
4. The fracture toughness parameters are calculated from the load, displacement and initial crack length.

1.4.1 K_{Ic} testing

(a) Types of test piece

Two main types of test pieces are recommended.

(i) Bend test pieces: These are the simplest and cheapest to machine. Limitations are imposed upon the test piece dimensions and the shape and depth of the notch. The pieces most commonly used have $B = \frac{1}{2} W$, $a = 0.45\ W$ to $0.5\ W$, where

B is the thickness, W is the width and a the crack length of the specimen.

(ii) Compact tension test pieces: The specimen tension test pieces use less material, but the cost of machining the clevis pinholes accurately is considerable. The recommended dimensions are $B = \frac{1}{2} W$, $a = 0.45$ to $0.55\ W$ and $2F = 0.275\ W$. Please refer to Figure 8.

(b) Testing Fixtures

To reduce friction to a minimum, bend tests are made on freely rotating rollers with or without fixed centres. The diameter of the rolls and centre of loading point should be between $\frac{1}{3} W$ and W.

(c) Test piece dimensions

The plane strain fracture toughness of a material is a measure of its resistance to unstable fracture under conditions where plastic deformation is limited to a region of the crack tip which is small in comparison to the test piece size, but the manner and the degree in which plasticity is to be limited is confirmed recently.

This is achieved by restricting the nominal stress at the crack tip to below the yield stress. The nominal stress is the stress that would exist at the crack tip if there were no stress intensification there.

In a compact tension test piece:

$$\sigma_{nom} = \frac{2Q(2W + a)}{B(W - a)^2} \qquad (21)$$

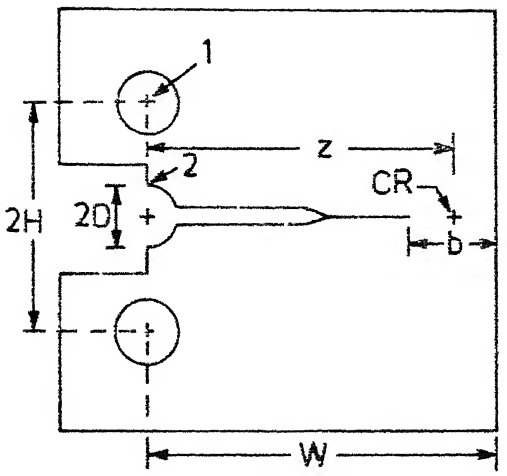

Fig. 8. Schematic of compact specimen. 1, load point; 2, displacement point; CR, centre of rotation.

and in a bend test piece:

$$\sigma_{nom} = \frac{3QL}{B(W - a)^2} \qquad (22)$$

where Q is the applied load.

ASTM special committee has accepted the recommendation that the nominal stress should not exceed 0 percent of the 0.2 percent proof stress.

Another requirement is that is to limit plastic deformation by maintenance of plane strain conditions at the crack tip. According to the standardized procedure to ensure plane strain ASTM 24, consistent K_{Ic} values could be obtained if

$$a, B > 2.5 \left(\frac{K_{Ic}}{\sigma_y}\right)^2 \qquad (23)$$

where a is the crack length

B is the thickness of the test piece.

Moreover a/W values greater than 0.55 were considered undesirable because at high a/W values small errors in crack length can give rise to large errors in K_{Ic}.

(d) Fatigue pre-cracking

Basic requirements for the fatigue pre-cracking:

(a) The ratio of minimum to maximum force shall be in the range of 0 to 0.1.

(b) K_f shall not exceed 0.7 $(\sigma_{y_1}/\sigma_{y_2})K_Q$ where σ_{y_1} and σ_{y_2} are the proof stresses at the

temperatures of fatigue cracking and at the test temperature respectively.

(c) The crack length shall be not less than 1.25 mm and the a/W ratio shall be in the range 0.45 to 0.55.

After testing the crack is measured and the effective crack length is measured from the average of three measurements at 25, 50 and 75 percent B.

(e) Instrumentation

A fracture toughness test is conducted in much the same way as a tensile test, the extensometer to measure strain being replaced by a gauge located across the notch of the test piece to measure the crack opening displacement.

(f) The offset procedure

K_{Ic} values were originally calculated from the pop-in load illustrated in Figure 9. Type IV since many materials do not exhibit pop in a procedure is established to determine K_{Ic} values from force-displacement records showing deviations from linearity but no sudden discontinuity i.e. type I, Figure 9. The secant intercept procedure is adopted for this purpose.

The procedure is as follows. Referring to Figure 9 draw the secant line OQ_5 through the origin with slope 5% less than the tangent OA to the initial part of the record. Draw a horizontal line representing a constant force of 0.8 Q_Q; q_i is the distance along this line between OA and the curve record. If this deviation from linearity at the

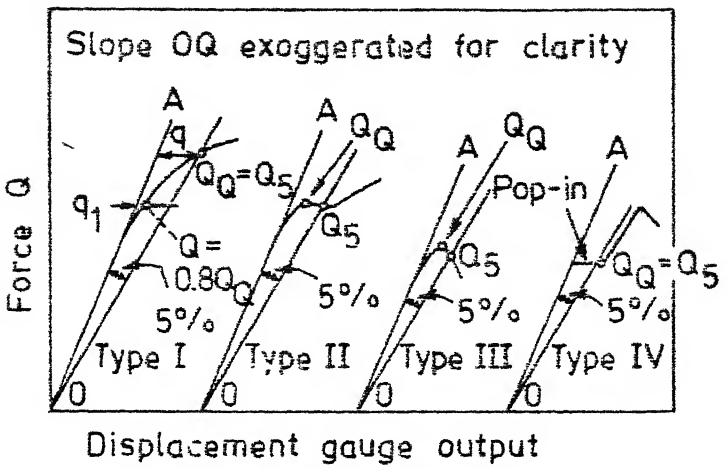

Fig. 9 Schematic force/displacement records showing quantities involved in analysis.

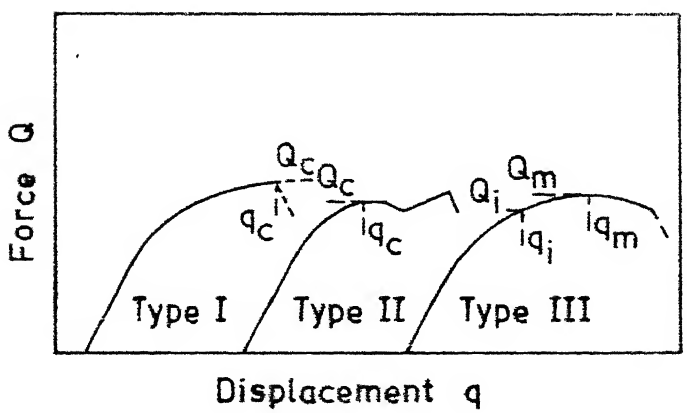

Fig. 10. Force/displacement records for calculation of COD.

force of 0.8 Q_Q is more than 1/4 of the corresponding deviation, q, at the force of Q_5 excessive non-linearity is present and so the curve is rejected.

So, for this situation the test piece of greater thickness should be selected and the experiment is to be repeated for K_{Ic}.

(g) Calculation of K_{Ic}

The stress intensity factor at the tip of a crack of length 2a, for the three point bending is given by

$$K = \frac{QY}{BW^{1/2}} \qquad (24)$$

where Y is the compliance function derived from the relationship between test piece compliance and dimensionless crack length a/W i.e.

$$Y = f(\frac{a}{W})$$

$$= 1.93(\frac{a}{W})^{1/2} - 3.07(\frac{a}{W})^{3/2} + 14.53(\frac{a}{W})^{5/2} - 25.11(\frac{a}{W})^{7/2} + 25.80(\frac{a}{W})^{9/2} \qquad 25$$

These values are given in tabular form for values of a/W between 0.45 and 0.55 in increments of 0.001(a/W).

1.4.2 COD testing

Both COD and K_{Ic} tests are performed using a unified testing procedure and therefore employ similar test pieces, fatigue pre-cracking procedures, testing procedures and analysis.

The crack opening displacement is a measure of the resistance of materials to fracture initiation under conditions where gross plastic deformation occurs and linear elastic fracture mechanics becomes invalid. The main objective of the COD test is to determine the critical crack opening displacement at the tip of a sharp crack at the onset of crack extension. This is done by measuring the displacement at the mouth of the notch using a gauge identical to that used in K_{Ic} tests and by performing a suitable calculation.

Testing

The test record consists of a plot of force Q versus crack opening displacement at the notch mouth measured by a displacement transducer. A typical record is shown in Figure 10 where the critical displacement q_c at instability is the total value corresponding to the maximum applied force Q_c, Figure 10. In the case of type II, if the falling load portion can be shown to be associated with crack growth, by electrical potential method or by an audible sound, then Q_c is measured at the discontinuity shown. The third type of record where there is no sudden discontinuity is associated with slow crack growth which commences during the rising portion of the test record. An electrical potential method must be used to detect at the initiation of stable crack growth δ_i.

In those cases where crack growth cannot be measured the crack opening displacement δ_m at the

displacement q_m corresponding to the first attainment if a maximum load can be used.

Several methods have been proposed for converting q_c values to δ_c and used in practice.

1.4.3 J-determination techniques

i) Compliance J

The J-integral can be conveniently evaluated through the energy release rate interpretation of J as derived by Rice [14]. As explained earlier, J may be written for non-linear elastic material with no crack advance as:

$$J = -\frac{1}{B}\frac{\partial u}{\partial a}\bigg|_u = \frac{1}{B}\frac{\partial c}{\partial a}\bigg|_F \qquad (26)$$

where F is the applied load

u is the load point displacement and

c is the complementary energy $\int q\, dF$.

In the case of plasticity, where deformation is irreversible and J cannot be interpreted as the energy available to drive the crack, the contour integral J is numerically equal to

$$-\frac{1}{B}\left(\frac{\partial u_{el}}{\partial a}\bigg|_u + \frac{\partial u_{pl}}{\partial a}\bigg|_u\right) \qquad (27)$$

This represents the energy difference for monotonically loaded cracks cut initially to different lengths.

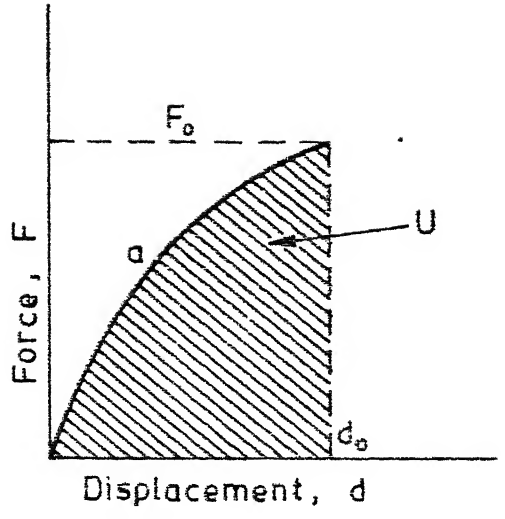

(a)

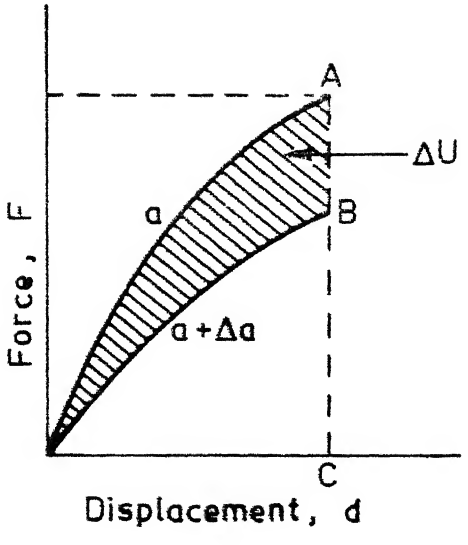

(b)

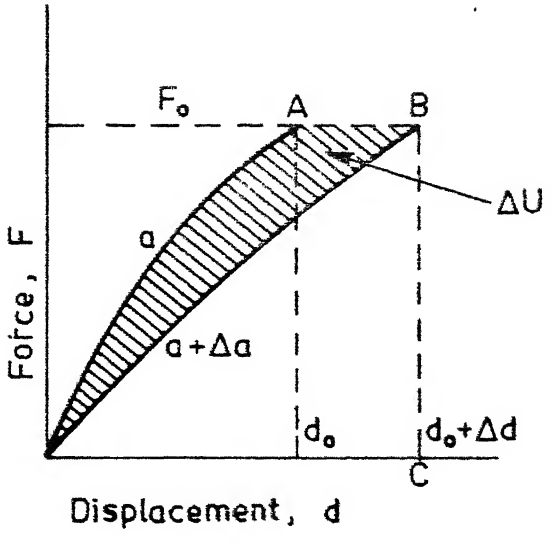

(c)

Fig. 11. Schematic load - displacement curves with prescribed load / displacement.

Using equation (26) J may be experimentally evaluated as follows. For convenience displacements are prescribed as boundary conditions. Hence, the second term of the J integral in equation (18) drops out i.e., the potential energy becomes equal to the integral of the strain energy which is simply equal to the work done on the body.

The J-integral can be evaluated considering the load deflection diagrams of similar bodies with neighbouring crack sizes. When two similar bodies with crack lengths a and $a + \Delta a$ are loaded, the load deflection curves are represented by OA and OB. If in the first body, the crack extends from a to $a + \Delta a$ under prescribed load F_o, the total work done on the body is represented by the area OABCO (Figure 11(b)). Because of reversibility, the unloading curve from the point B is the same as the loading curve of the body starting with a crack length, $a + \Delta a$. The strain energy of the body with a crack length $a + \Delta a$, under the load F_o is the area OBCO. The shaded area OAB0 $(-\Delta U)$ is the energy available for crack extension. Similarly when the crack extends from a to $a + \Delta a$ under prescribed displacements, the energy available for crack extension is the shaded area OAB0 (Figure 11(b)).

At any given displacement, the area under the load versus load point displacement record may be found for bodies with different crack lengths. The slope of the plot U versus 'a' at a given displacement is $\frac{\partial U}{\partial a}\Big|_v$ and hence J can be determined. This process is shown schematically

in the Figure 12. The final plot is J versus the applied displacement. In general, this curve depends on the crack length a. If the applied displacement is found for the initiation of crack growth, the critical J value, J_{Ic} may be found.

ii) J_{Ic} testing using Rice et al estimation procedures

A compliance determination of J, while possessing the advantage of generality, is tedious and expensive in both time and material and therefore is no longer used to determine experimentally. A significant advance in fracture toughness testing was provided by the development of the Rice-Paris-Merkle J formula for deeply cracked bars subjected to bending [19]. This same method has been made use of in our present study of the determination of J for the low alloy steel.

a) The Rice-Paris Merkle J

The derivation of this formula is based on the fact that the angle of bend θ, for deeply cracked bars, is only a function of the applied moment M and the square of the remaining ligament, b (Ref. Figure 13)

$$\theta = f\left(\frac{M}{b^2}\right) \tag{28}$$

Using the potential energy definition of J given by equation (26) and the fact that da is equal to -db, J can be written as

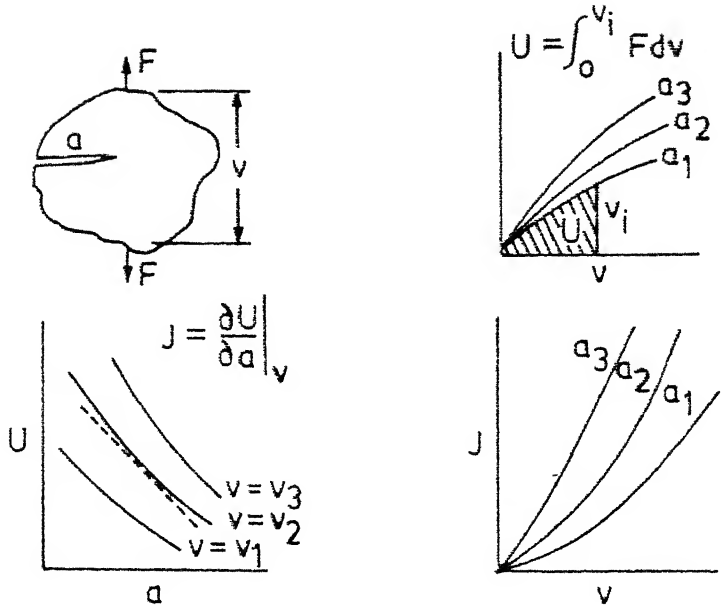

Fig 12. Schematic of steps in a compliance J determination.

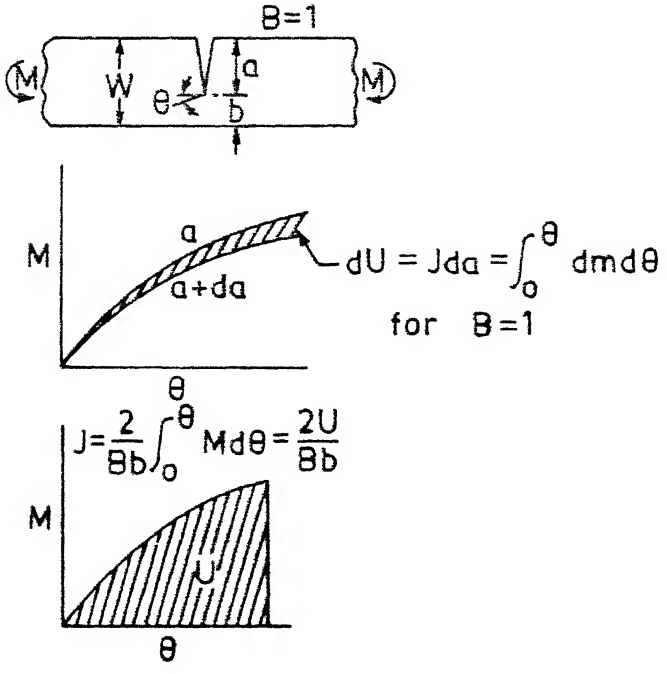

Fig. 13. Schematic showing Rice-Paris-Merkle J formula for bend type specimen.

$$J = \frac{1}{b}\int_0^{\theta} \left.\frac{\partial\theta}{\partial a}\right|_N dM$$

$$= -\frac{1}{B}\int_0^{\theta} \left.\frac{\partial\theta}{\partial b}\right|_M dM \qquad (29)$$

This is schematically illustrated in Figure 13. From equation (14)

$$-\left.\frac{\partial\theta}{\partial b}\right|_M = -f'\left(\frac{M}{b^2}\right)\left.\frac{\partial(M/b^2)}{\partial b}\right|_M = \frac{2M}{b^3} f'\left(\frac{M}{b^2}\right) \qquad (30)$$

similarly

$$\left.\frac{\partial\theta}{\partial M}\right|_b = \frac{f'(M/b^2)}{b^2} \qquad (31)$$

and thus

$$-\left.\frac{\partial\theta}{\partial b}\right|_M = \frac{2M}{b}\left.\frac{\partial\theta}{\partial M}\right|_b \qquad (32)$$

Substituting equation (32) in equation (29)

$$J = \frac{2}{Bb}\int_0^{M} M \cdot \left.\frac{\partial\theta}{\partial M}\right|_b dM$$

$$= \frac{2}{Bb}\int_0^{\theta} M\, d\theta \qquad (33)$$

yields the result that J is simply related to the work done on the specimen. Again the above derivation holds true for deeply cracked bars in bending such that θ is only a function of M/b^2. The concept of relating J to the work done on the specimen is one that is used almost exclusively in present test methods.

b) Testing procedure

From the discussion above, it is learnt that this method is based on the approximate formulation for calculating J given by Rice et al

$$J = \frac{2A}{Bb} \tag{34}$$

where B = specimen thickness

b = remaining uncracked ligament of the specimen,

and A = area under the load versus load point displacement curve.

This formulation applies to a specimen with a deep crack subjected to a bend type of loading. The types of specimens most suited to this formulation are the compact toughness specimen (CT) and bend bars with three point loading.

The method proposed for determining the J_{Ic} measurement point is shown schematically in Figure 14. Several identical specimens are loaded to differing values of displacement and then unloaded (Figure 14(a)). These specimens will hopefully all exhibit different amounts of crack growth. After unloading, the crack advance is marked and the specimens broken open so that the crack advance, Δa, can be measured (Figure 14(b)). Different methods can be used to mark the crack advance. For steels the easiest method is heat tinting. The specimens are heated about 600°F for about 10 min. The specimens subsequently are broken open at liquid nitrogen temperature. The value of J at the point where the specimen is unloaded is determined

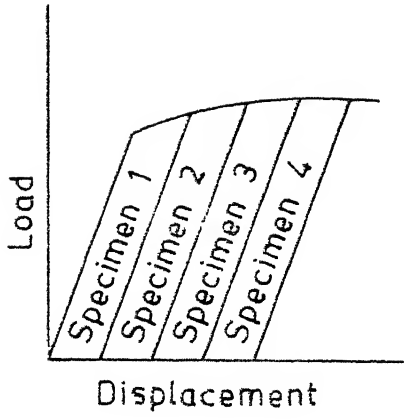

(a) Load identical specimens to different displacements.

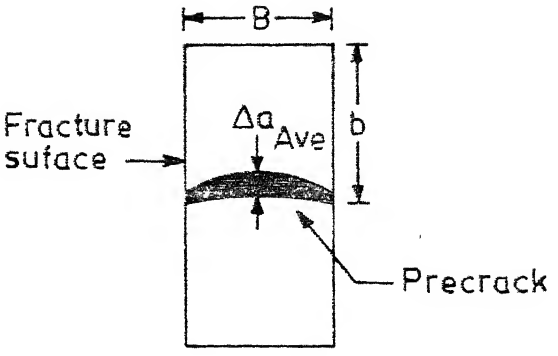

(b) Heat tint and measure average crack extension

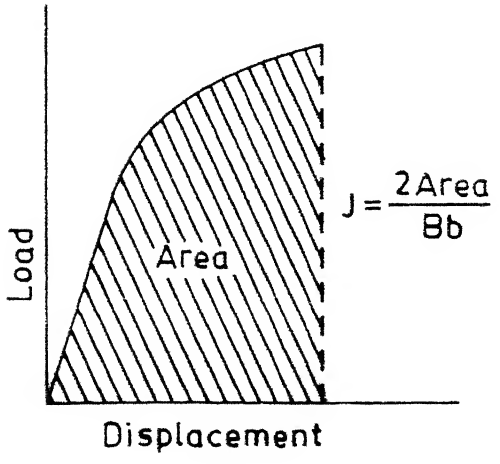

(c) Calculate J for each specimen

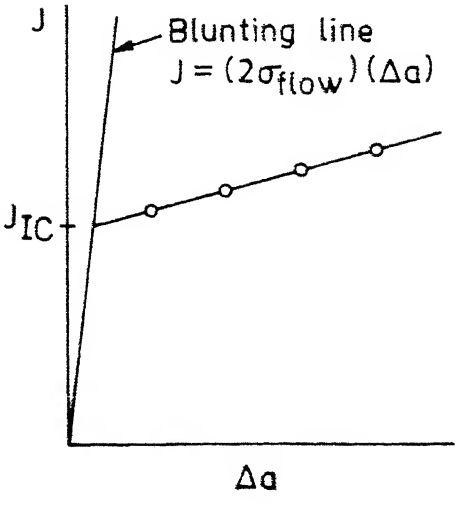

(d) Plot J vs Δa find J_{IC}.

Fig. 14. Procedure for experimental J_{IC} measurement: multiple specimen R-curve.

from equation (20) for each specimen (Figure 14(c)). This value of J is plotted as a function of crack advance (Figure 14(d)).

The curve in Figure 14(d) is the crack growth resistance curve from which J_{Ic} is determined. The present method for determining J_{Ic} uses the blunting line define as

$$J = 2\sigma_{flow}\Delta a \qquad (35)$$

the point where additional crack advance occurs from the blunted crack, that is, the J_{Ic} measurement point, is marked by a change of slope in the curve of J versus crack extension. The points on the plot which lie to the right of the blunting line are generally filled with a straight line and J_{Ic} is taken at the intersection of this fitted line and the blunting line.

The method for determining J_{Ic} as described by Figure 4 is presently used as a standard method. Certainly some aspects of this method can be improved. Most notably perhaps is the method of analysing the data points in Figure 14(d) to obtain J_{Ic}. This analysis is somewhat subjective and can possibly lead to ambiguous values of J_{Ic}. The use of the approximation formula from equation (34) has been compared experimentally with the original energy rate definition of J, equation (3) and found to compare favourably for $a/W > 0.6$.

Fatigue pre-cracking of specimens:

Specimens should be precracked in fatigue with a maximum permissible load not exceeding one fourth P_L, which can be calculated from the following

$$P_L = (\frac{4}{3}) \frac{B\, b^2\, \sigma_{flow}}{S} \quad \text{for the bind specimen} \qquad (36)$$

where b is uncracked ligament, B is the specimen thickness, S is the specimen bend span and σ_{flow} is the flow stress. Fatigue cracking should be conducted at a sufficiently low load so that the crack tip is not overloaded. The J_{Ic} test is expected to go into the plastic regime which means that specimen will most probably reach limit load.

c) Limitations of this J_{Ic} testing

One important limitation on the test method is specimen size needed to determine a J_{Ic} value. This size limitation is generally expressed by

$$B,\ a \quad \geq \quad \alpha\ J_{Ic}/\sigma_{flow} \qquad (37)$$

where B, a, are the specimen thickness, crack length respectively. α is a non dimensional constant taken to be somewhere in the order of 25 to 50. These values in fact differ from one material to another depending on such things as the degree to which the material strain hardens.

Another important limitation on the use of the present J_{Ic} test methodology lies in the specimen type. The

approximation formula for J given by equation (34) has been formulated only for bend type specimens. Although approximations exist for other types of specimens, care should be exercised whenever a specimen other than a CT or bend bar is used.

1.4.4 New test methods

With the use of equation (34) J can be determined for a single specimen at any given value of displacement. To determine the whole curve of J versus Δa hence J_{Ic} from a single specimen all that is needed is a continuous monitor of crack advance during the generation of the load-displacement curve. Several methods have been demonstrated which can accomplish this successfully. They are namely elastic compliance method, electrical potential method and ultrasonic method.

CHAPTER II

EXPERIMENTAL PROCEDURE

The HSLA steel used in the present investigations had the following composition:

Chemical composition, weight %

C	Mn	P	S	Si	V	Mo	Ce
0.13	0.75	0.023	0.025	0.09	0.12	0.20	8.8

The regular mechanical properties of the steel were determined using standard tensile test specimens recommended by ASTM and tabulated below. A micrograph of the steel under study in as received condition is shown in the next page.

Mechanical properties		
0.2% yield strength	-	430 MN/m^2
Ultimate strength	-	525 MN/m^2
Elongation	-	27%
Room temperature charpy energy	-	13 ft-lb

Bend tests, direct tensile tests and charpy impact tests were carried out over a range of temperatures in order to correlate fracture toughness with other mechanical properties.

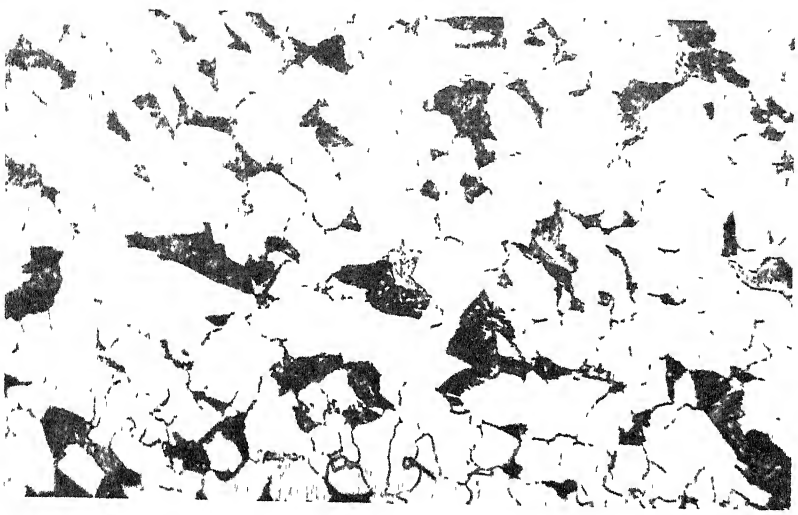

Microstructure of the HSLA steel in as received condition

2.1 BEND TEST

2.1.1 Specimen design and preparation

Specimens (100 mm x 20 mm x 10 mm) for the three-point bend test were machined from the as received angle.

a) Plane strain condition: One important requirement of this test method is to limit plastic deformation by maintaining of plane strain conditions at the crack tip. High triaxial stresses are developed at the crack tip, if the test piece is thick which prevents spreading of yield laterally to the centre of the crack-front. The size requirement for test specimens to ensure plane strain is given by the relation

$$B, a \geq \alpha J_{1c}/\sigma_{flow}$$

where B, a are the specimen thickness, and crack length respectively. σ_{flow} is the flow stress which is taken as the average of yield stress and ultimate stress. α is a non dimensional constant taken to be in the order of ~25. This value might differ slightly from one material to another depending on the degree to which the material strain hardens.

Different specimens of varying thickness and crack length were produced and tested and the values of J_{1c} and σ_{flow} analysed. The dimensions of the test samples were thus made consistent with the bar criterion. The

standard bend type specimens were prepared according to J_{1c} test standard E813-81 ASTM. The sample had the profile and dimensions as shown in Figure 15.

The loading conditions of the specimen during the test is shown in the Figure 16.

b) Specimen preparation: Many specimens of the dimensions 100 x 20 x 10 mm were machined from the angle. The crack length to width of the specimen ratio i.e. a/W was kept 0.75 in all the specimens. First, a slot of 1 mm width and 13 mm length was made in each specimen on the full thickness and along the width direction of the specimen. This was done uniformly by milling in all the specimens. The final 2 mm of the required 15 mm notch depth was cut by a spark erosion wire. The spark erosion machine (Model No.) used paraffin as the dielectric medium and operated at a minimum gap voltage to prevent overheating of the crack root. The speed of cutting was also kept low to create smooth cutting.

Similar notches were cut in all the specimens used in the bend tests. The a/W ratio was kept consistent at 0.75 in all the specimens. The radius of the root of the notch was measured by shadow graph as 0.6 mm

All the specimens were polished on all the sides and were free of any surface defect, before testing on the bending fixtures.

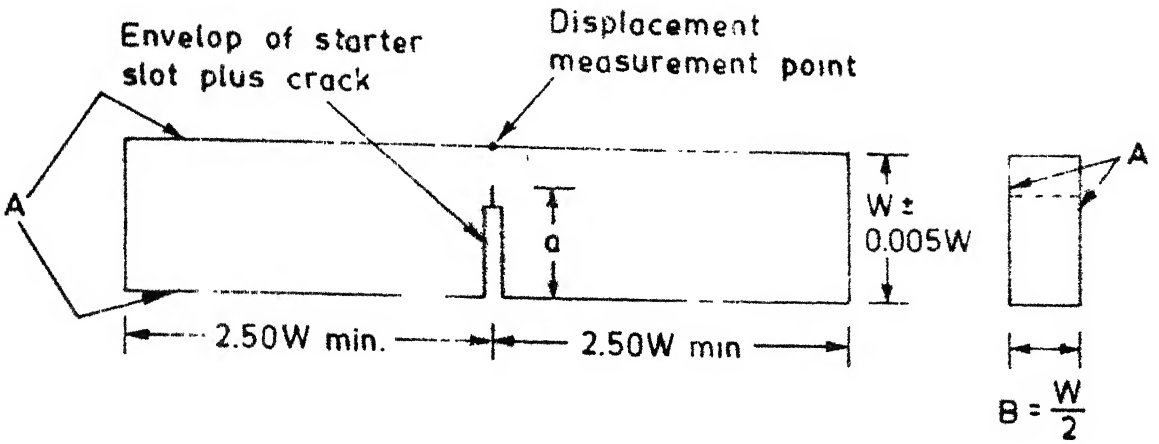

W = 20 mm
B = 10 mm
a = 15 mm, $\frac{a}{W}$ = 0.75

Fig. 15. Bend specimen Standard proportions and tolerences. Surface A is perpendicular and parallel to within 0.001W crack is perpendicular to specimen length and thickness to within 2°.

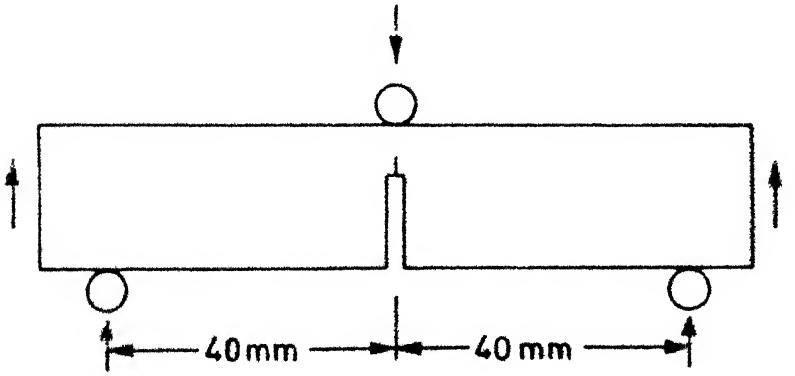

Fig. 16. Loading conditions of the specimen during bend test.

2.1.2 Test procedure

Bend tests were carried out in a MTS floor model machine of the hydraulic arm movement type. The standard bending fixtures were fixed on the MTS. Initially a test was conducted at room temperature. A specimen was mounted on the fixture and the bottom rolls were adjusted to give the required span length of exactly 80 mm. The point of application of the load, P, on the specimen was properly fixed with the help of a telescopic viewer. The cross head motion was fixed at the rate of 1.5 mm/sec. Proper scales were chosen for the load and displacement measurements on the X-Y recorder. A plot between load and the displacement of load point was obtained. The test was stopped once the load dropped due to the initiation of the crack and the point of maximum load was pin-pointed. The area under the curve, A i.e. measured till the maximum load, gives the work done on the specimen to initiate the crack. This area as described earlier related to the J-value by the equation

$$J = \frac{2A}{Bb}$$

B is the specimen thickness and
b is the uncracked ligament.

Correction of load displacement records

Several sources of coincidental displacement are included when load displacement in three-point bending is measured from the loading pin relative to the test base.

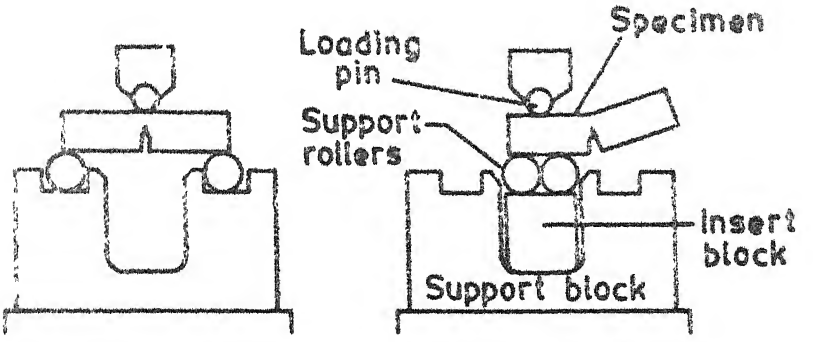

(a) Specimen in standard testing position.

(b) Specimen in position for post-test determination of displacement correction using insert block.

Fig. 17. Bend test apparatus with specimen in position for testing and for correction determinations after the test.

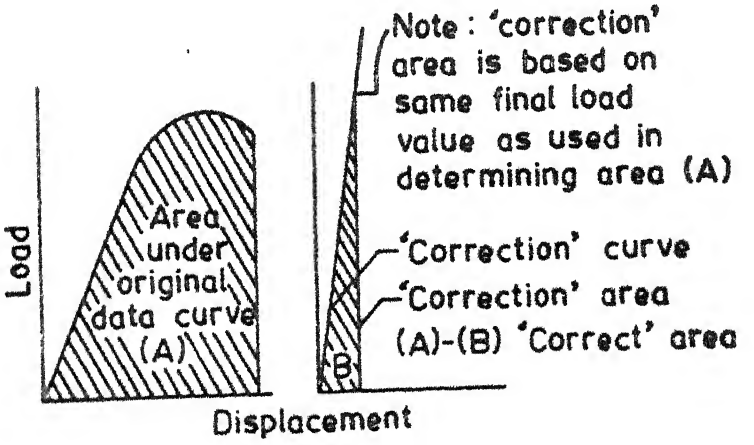

Fig. 18. Methods of applying correction for coincidental displacement to load-displacement record.

The major errors are due to elastic deformation of the various test fixture components and the elastic and plastic indentations of the specimen by the loading pin and supporting rollers. A method for correcting the test record for such coincidental displacement has been discussed by R.J. Buzzard and D.M. Fisher [20]. The experimental set up for determining coincidental load point displacement is illustrated in Figures 17 and 18

A block of the same material and material condition as the support block was inserted into the span gap of the support block. The support rollers were butted together to provide a span as close to zero possible. An undeformed part of the test specimen is then placed in position on the butted rollers with the some orientation as in the test proper. A load versus load point deflection record was obtained as described in the previous section with the highest load slightly in excess of the maximum load achieved during the bend test. This is schematically described in Figure 17.

In determining J_i, the test record was primarily used to obtain the area under the load-displacement curve. A simple and direct method used for determining the corrected area under a load-displacement curve is depicted in Figures 17 and 18. The area under the coincidental displacement curve was simply substracted from the area under the primary test curve to yield the corrected area for the test.

No replotting is necessary in using this procedure, thus conserving much time and effort in analyzing test data.

2.1.3 Bend tests at various temperatures

The bend tests were carried out at various temperatures including both sub-zero and high temperatures in a floor model MTS. The aim was to determine the temperature dependence of J_1. Tests were conducted at $-170 \pm 20°C$; $-59 \pm 6°C$, $-21 \pm 4°C$; $-10 \pm 3°C$; $101 \pm 3°C$; $28°C$; $190 \pm 8°C$; $260 \pm 15°C$ and $340 \pm 20°C$.

Suitable thermocouples i.e. copper-constantan thermocouple for sub-zero temperatures and Chromel-Alumel thermocouple for high temperatures, were soldered to each specimen. For the sub-zero temperature tests, samples were soaked at liquid nitrogen for more than 10 minutes. The specimens were then taken out and fixed on the bending fixtures as quickly as possible and the temperature monitored continuously. The test was started when once the required temperature was going to be reached. In each test, the temperature was noted at the point when the load dropped after reaching the maximum load and the test was stopped and specimen taken out. The total duration of the test was limited to 1-2 minutes. But the strain rate remained constant for all the temperatures.

Similar procedures were also carried out for higher temperature tests. Specimens were soaked in a furnace at about 600°C for 10 minutes and removed quickly for the test and temperature monitored during the test. The test was

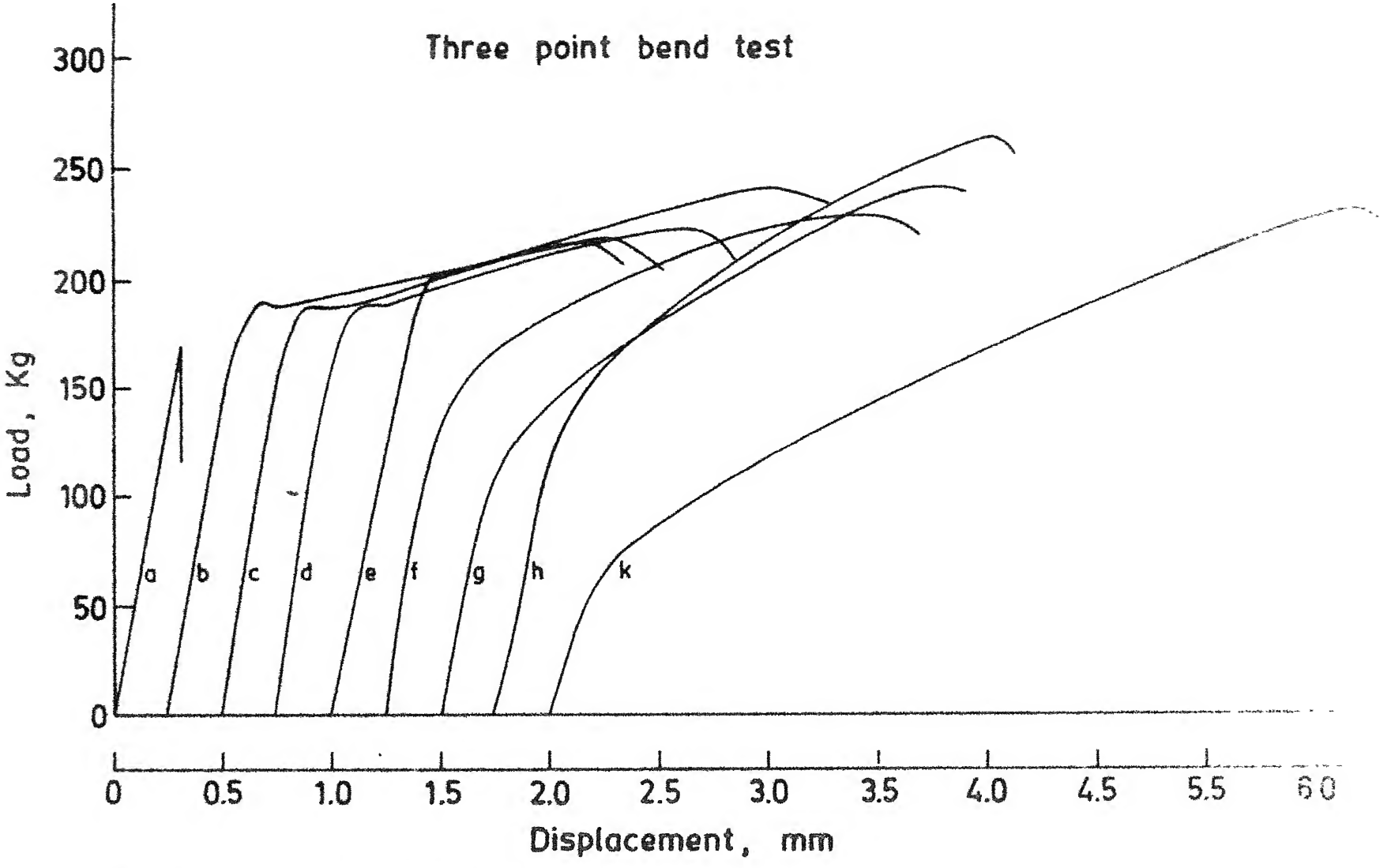

Fig. 20. Load displacement records for three point bend tests at various temperatures (a)-170°C (b)-59°C (c)-21°C (d)-10°C (e) 28°C (f) 101°C (g) 190°C (h) 260°C

stopped as before by noting the temperature at load drop. The divergency in the mean test temperature was thus obtained for all temperatures, from the temperature at the commencement of test and the finish temperature.

The cross-head speed and correspondingly strain rate was kept constant for all tests carried out at different temperatures. The load-displacement records were plotted on a separate X-Y recorder and the corresponding areas under load-displacement plot were determined. From these areas the coincidental displacement area (discussed above) was subtracted to obtain the respective 'corrected areas'.

The J-values were calculated using the relation

$$J = \frac{2A}{Bb}$$

where A is the area under load displacement

B is the thickness

b is the unbroken ligament.

'or the different temperatures. Then these J-values were plotted against temperature (Figure 21), and the results analysed.

2.2 STRAIGHT TENSILE TEST

Tensile specimens of the same steel were machined according to the dimensions shown in the Figure 19. Straight tensile tests were carried out at temperatures 30°C (RT), 130°C ± 2; 180°C ± 2; 222°C ± 2; 250°C ± 2; 400°C ± 2. The tests were conducted in the floor model Instron 1195. The

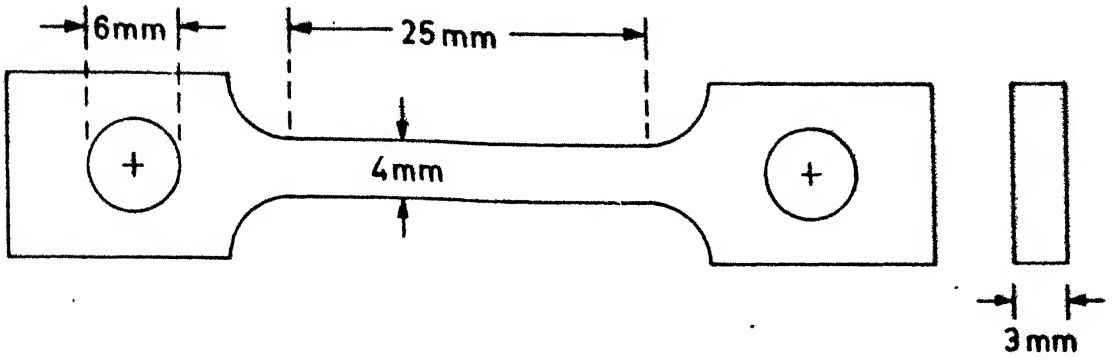

Fig. 19A. Profile and dimensions of direct tensile test specimen.

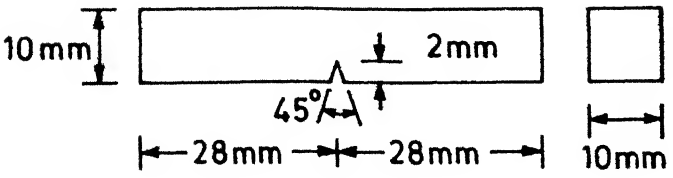

Fig. 19B. Charpy impact test specimen.

specimens were mounted on a specially designed grips. The furnace temperature was brought to the required one and specimen along with the grips were introduced inside and properly mounted at both ends. Once the specimen attained the required temperature which was again monitored by a thermocouple attached to its centre, the test was conducted. Generally, it took around 10 minutes to soak to the required temperature before the test started. A cross-head speed of 1 mm/min corresponding to a strain rate 6.67×10^{-4} sec^{-1} was used at all temperature tests. The load-displacement plots were obtained for all the specimens at different temperatures and converted into engineerins stress versus engineering strain plots after applying machine corrections. All these plots have been presented in Figures 22(a-f).

2.3 NOTCHED BAR IMPACT TEST

Standard Charpy-test were carried out using notched test bars at a range of temperatures from -130°C to 400°C. The dimensions of the test specimen are given in Figure 19. The specimen has a square cross section (10 mm x 10 mm) and contains a 45°V notch, 2 mm deep with a 0.25 mm root radius. The specimens were soaked in liquid nitrogen for sub-zero temperature tests and soaked in the furnace at 600°C for high temperature tests. The specimens were taken out of the respective soaking medium and tested once the specimens reached the test temperatures while on the anvil of the Impact machine. The impact values are tabulated in the next

chapter and are graphically plotted in Figure 21 as impact energy versus temperature

CHAPTER III

RESULTS AND DISCUSSION

3.1 BEND TEST RESULTS

The J_1 values calculated from the load-displacement plots of the bend test, carried out at different temperatures are tabulated as follows:

Temperature, °C	J_1/KJ/m^2
-170	12.82
- 59	45.01
- 21	140.07
- 10	168.92
28	190.70
101	195.20
190	186.51
260	213.00
340	268.59

These results have been graphically plotted taking J_1 values an ordinate and temperature on abcissa. This is shown in Figure 21. From this graph it is obvious that J_1 values increase with temperature from sub-zero temperatures to higher temperature level. This indicates that the fracture toughness of the steel under investigation increases with temperature. There is a sharp decrease in the

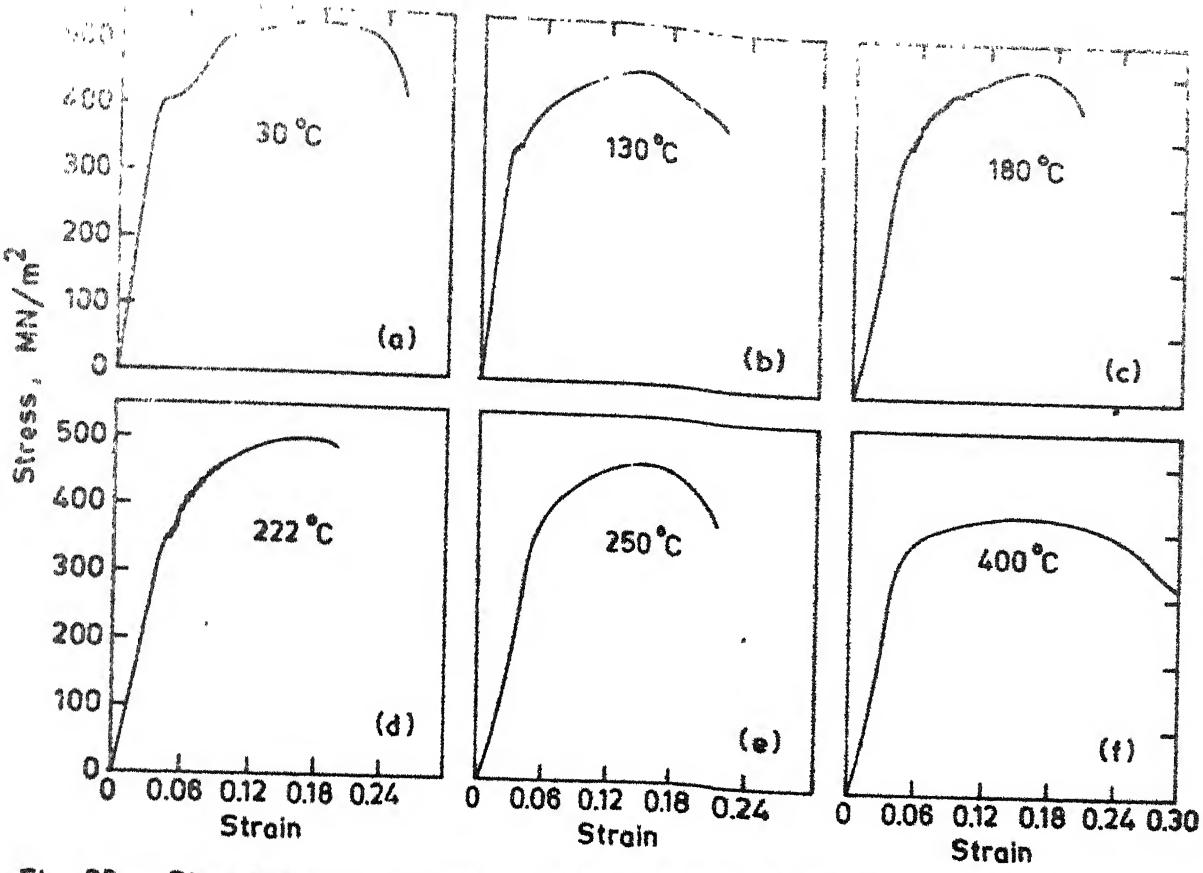

Fig. 22. Stress strain curves of direct tensile tests at various temperatures.

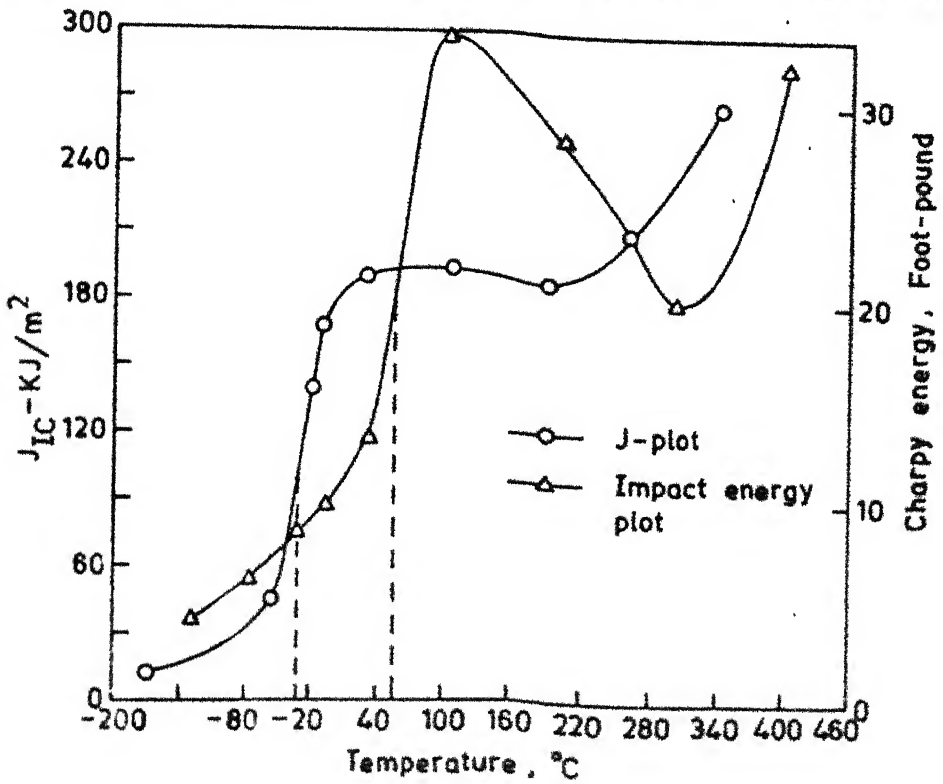

Fig. 21. Fracture curves
(i) J vs temperature
(ii) Impact energy vs temperature plot.

Secondly, the occurrence of brittle fracture is associated primarily with the body-centred cubic metals. This is more pronounced in the presence of impurities which form interstitial solid solutions. The most important element is carbon in α-iron which, even if present to the extent of only a few parts per million, will cause the metal to undergo a ductile-brittle transition.

The main role of the interstitial impurity atoms is the introduction of a sharp yield point in the stress-strain curve. This is a result of the strong asymmetric distortion which these atoms produce in the b.c.c. structures which causes them to have a large interaction energy with the stress fields of dislocations. Strong dislocation locking will take place, so that when plastic deformation occurs it will be either by the sudden avalanche of dislocations which are torn from their solute atmospheres, or by the rapid movement of newly generated dislocations, which have no solute atmosphere. In either case, the conditions are suitable for the coalescence of dislocation to form crack nuclei, for the first dislocations to move are acted on by a high stress, and thus will have high velocity. As the temperature is lowered, the yield stress rises steeply which is again a characteristic of b.c.c. metals. In terms of dislocations this means that Peierls-Nabarro stress in b.c.c. metals is strongly temperature dependent. Consequently, first dislocation to be mobile will move more rapidly at lower

temperatures, and the chances of forming crack nuclei will increase.

Sometimes twins are also responsible in the nucleation of cracks. Another point to be considered is that the marked temperature dependence of flow stress makes plastic deformation at the tip of the crack more difficult as the temperature is lowered. Thus at low temperatures there will be less plastic blunting of the crack, and propagation will occur more readily.

a) Ductile-brittle fractures: A brittle fracture is characterized by separation normal to the tensile stress. Outwardly there is no evidence of deformation. A clevage fracture appears bright and granular, owing to the reflection of light from the flat cleavage surfaces. The process of brittle fracture consists of (i) plastic deformation involving the pile-up of dislocations along the slip plane at an obstacle, (ii) the build up of shear stress at the head of the pile-up to nucleate a micro-crack, (iii) sometimes stored strain energy drives the micro-crack to complete fracture without dislocation movement in the pile-up. In metals, a distinct growth stage is observed in which increased stress is required to propagate the micro-crack.

A ductile fracture is characterized by a 'cup and cone' type separation. Necking begins at the point of plastic instability where the increase in strength due to strain hardening fails to compensate for the decrease in

cross sectional area. The formation of a neck introduces a triaxial state of stress in the region. Many time cavities form in these region and under continued straining these grow and coalesce into the central crack. This crack grows in a direction perpendicular to the axis of the specimen until it approaches the surface. It then propagates along localized shear planes at roughly 45° to the axis to form the 'cone' part of the fracture. The voids which are the basic source of ductile fracture are nucleated heterogeneously at sites where compatibility of deformation is difficult such as inclusions, second-phase particles, grain boundaries etc.

The process and reasons discussed above hold true for the bend test we have conducted to estimate J values at different temperatures. The brittle and ductile failures of the bend specimens have the same reasoning mentioned above.

b) Effects of notch in the fracture behaviour: Bend specimens here contain notches. The changes produced by the introduction of a notch have important consequences in the fracture process. The presence of a notch will alter the ductile to brittle transition of steel. A notch creates a local stress peak at the root of the notch producing triaxial stresses. Plastic flow begins at the notch root when this local stress reaches the yield strength of the material. As a result of this general yield stress of a notched specimen is greater than the

uniaxial tensile stress σ_o because it is more difficult to spread the yielded zone in the presence of triaxial stresses.

The triaxial stress state of a notch results in 'notch strengthening' in a ductile metal, but in a material prone to brittle fracture the increased tensile stresses from the plastic constraint can exceed the critical value for fracture before the material undergoes general plastic yielding.

Another effect of the notch is to produce high, locally concentrated strain. The accompanying strain hardening can lead to ductile void formation that can become converted into brittle cracks. In summary, a notch increases the tendency for brittle fracture in four important ways:

By producing high local stresses
By introducing a triaxial tensile state of stress
By producing local strain hardening and cracking
By producing a local magnification to the strain rate.

The whole discussion above is intended to explain the behaviour of J versus temperature dependence curve (Figure 21) where a brittle to ductile transition is shown by a sudden increase in the J values.

3.2 TENSILE TEST RESULTS

From the J versus temperature curve, it is observed that there exists a plateau region between B and C

i.e. in the temperature range of 30°C (R.T.) - 230°C. There is not much change in the values of J in this temperature range.

Straight tensile tests were carried out at six different temperatures thus scanning the whole range of the fracture curve from room temperature to high temperatures. The results obtained are tabulated below:

Temperature, °C	% elongation	UTS/MN/m^2
30	27.09	525
130	20.16	474
180	20.00	505
222	21.20	502
250	22.16	480
400	29.29	420

The important finding in the present test is that of serrations that appeared in the load-displacement curve over the temperature range of 130°C-222°C.Corresponding to dynamic strain aging gives rise to a plateau in the J versus temperature curve. The occurrence of strain ageing is a fairly general phenomenon in metals. The reappearance of the yield point is due to the diffusion of carbon and nitrogen atoms to the dislocations during the ageing period to form new atmospheres of interstitials anchoring

the dislocations. Support of this mechanism is found in the fact that the activation energy for the return of the yield point on ageing in good agreement with the activation energy for the diffusion of carbon in alpha iron.

The serrations arise from successive yielding and ageing while the specimen is tested. If the speed of the dislocation is low, it may be able to move by dragging its atmospheres of impurities along behind it. At higher velocity the dislocation pulls away from the atmosphere and a yield drop occurs. Since the solute atom mobility is high at the temperatures at which discontinuous yielding occurs, new atoms move to the dislocations and lock them. The process is repeated many times, causing the serrations in the stress-strain curves.

For plain carbon steel discontinuous yielding occurs in the temperature regions of 100-300°C. Another interesting aspect of dynamic strain ageing is that when it occurs the yield stress of a metal tends to become independent of temperature. This is evident from the tensile curves plotted at different temperatures.

Thus it has been observed that the dynamic-strain ageing has a direct effect on the fracture criterion J. This is the reason for the plateau region of the curve in Figure 21. The serrations disappeared in the stress-strain curves above 250°C. So there is a corresponding change in the fracture curve also. J values again increase steeply above 250°C to 340°C.

Impact tests were carried out to properly understand the J_1 dependence on temperature. In the J_1 versus temperature plot a sudden decrease in the value of J_1 was observed in the temperature range -32°C and this was due to change in the mode of fracture from ductile to brittle one. The transition temperature was -32°C as observed in this plot. The corresponding transition temperature was also determined by direct Charpy impact tests carried out over the same temperature range and the results of the impact tests are given below.

3.3 IMPACT TEST RESULTS

Temperature, °C	Impact energy, ft-lb
-130	4
- 70	6
- 36	8
- 9	9
30	13
101	33
202	28
300	20
406	32

The principal measurement from the impact Charpy test is the energy absorbed in fracturing the specimen. The impact energy versus temperature plot shown in Figure 21 shows the transition region from ductile to brittle mode of fracture. In this plot we

observe that the energy absorbed increases with increasing temperature till 100°C. This increase does not occur sharply at certain temperature. This is due to the fact that there is no one constant temperature at which this ductile brittle transformation occurs for a given metal. The transition temperature is sensitive to a number of metallurgical variables of which purity and grain size especially with steels the heat treatment and even the steel-making practice are very significant variables.

In this plot, we note that the impact energy decreases from 33 ft-lb to 20 ft-lb in the temperature range of 100°C-300°C. This decrease in impact energy corresponds to the plateau region in the J versus temperature plot. This, we believe is due to the same reason stated before for the J curve i.e. the strain ageing phenomenon which occurs in this temperature range. This phenomenon is also called 'blue brittleness' generally observed in low carbon steels.

We observe from the Figure 21 that there exists a shift in the transition temperature from the J versus temperature plot to impact energy versus temperature plot. The shift is from -32°C to 55°C. This has been attributed to the strain rate effects in the two test procedures. In the impact test the specimen was forced to bend and fracture at a higher strain rate of the order of 10^3 sec^{-1} whereas in the bend test for J values strain rate was only 6.67×10^{-4} sec^{-1}. The transition temperature is sensitive to the

strain rate and so the shift in transition temperature is mainly due to the increased strain rate. Thus one has to be careful in using fracture toughness obtained from different test procedures as a design criterion.

3.4 COMPARISON WITH THE LITERATURE VALUES OF J_{1c}

Very little work has been done in this area since the method has been only recently approved and standardized. Consequently very little information is available.

The values obtained in our test compare well with the values obtained by others. The room temperature J_{1c} value 190 KJ/m^2 of our steel lies very well in the range of values obtained for high carbon steel to low alloy steel i.e. from 160 KJ/m^2 to 250 KJ/m^2.

Davis [21] had determined the J_{1c} values for two low alloy steels Ducol W30, B54360 50C which has alloying elements like Ni, Cr, Mo, V adding together amounts to ~2%. This steel had tensile strength of ~530 MPa and elongation 31%. Our steel does not differ much from these in terms of mechanical properties like these. His J_{1c} values range from 80 KJ/m^2 to 150 KJ/m^2 in the temperature ranges from -50°C to -20°C respectively. Our values vary from ~45 KJ/m^2 at -59°C to ~140 KJ/m^2 at -21°C.

Our values of J_1 at room temperature is also near to the value of Joyce [22]. He obtained the J_{1c} value for the type HY130 steel which is again a medium carbon low

alloy steel alloying elements like Ni, Cr, Mo and V amount to ~6%.

CONCLUSION

The concept of J-integral and the J-estimation through bend test procedure, thus well suited our study of J dependence on temperature. The tensile tests conducted over the temperatures corresponding to the plateau region in the J vs. temperature curve, clearly indicates that the dynamic strain ageing was responsible for this plateau region. Also the Charpy impact energy curve shows a drop in C_v values over this temperature range. The shift in the transition temperature from -32°C to 55°C between J-plot and impact energy plot may be attributed to the large difference in the strain rate effects.

There has been no work done in high carbon or low alloy steel to estimate the J value dependence on temperature. This work is a kind of first attempt to determine J dependence of temperature closely relating the behaviour to the material property. This is lot of scope for further investigation in this field.

REFERENCES

1. Griffith, A.A., 'The phenomena of rupture and flow in solids', Phil. Trans. Roy. Soc. 1921, A221, 163.

2. Orwań, E., 'Fracture and strength of solids', Rep. Prog. Phys. 1949, 12, 185.

3. Orwan, E., 'Fatigue and fracture of metals', Symp. at M.I.T., U.S.A., John Wiley & Sons, Inc., New York, 1952.

4. Irwin, G.R. and Kics, J.A., 'Fracturing and fracture dynamics', Weld. J. Res. Suppl. 1952, 17, 95S.

5. Irwin, G.R., 'Analysis of stresses and strains near the end of a crack traversing a plate', J. Appl. Mech. 1957, 24, 361.

6. Irwin, G.R., 'Fracture on encyclopaedia of physics', Vol. VI, Springer, Heidelberg, 1958.

7. Westergáard, H.M., 'Bearing pressures and cracks', J. Appl. Mech. 1939, 61, A49.

8. Irwin, G.R., 'Analysis of stresses and strains near the end of a crack traversing a plate', Trans. ASME, J. Appl. Mech. 24, pp. 361-4.

9. Wells, A.A. (1961), 'Unstable crack propagation in metals: Cleavage and fast fracture', Symp. Crack Propagation, College of Aeronautics, Cranfield, Paper B4.

10. Cottrell, A.H., 'Theoretical aspects of radiation damage and brittle fracture in steel pressure vessels', Iron and Steel Inst. Spec. Rep. 1961, No. 69, pp. 281-96.

11. Barenblatt, G.I., 'The mathematical theory of equilibrium cracks in brittle fracture', Adv. in Appl. Mech. 1962, 7, Academic Press, New York.

12. Dugdale, D.S., 'Yielding of steel sheets containing slits', J. Mech. Phys. Solids 1960, 8, 100-104.

13. Wells, A.A., 'Unstable crack propagation in metals: Cleavage and fast fracture', Crack Propagation Symposium, Cranfield, 1961.

14. Rice, J.R., 'A path independent integral and the approximate analysis of strain concentration by notches and cracks', J. Appl. Mech. 1968, 35, 379-386.

15. Hutchinson, J.W., 'Singular behaviour at the end of a tensile crack in a hardening material', J. Mechs. and Phys. of Solids 16, 1968, 13-31.

16. Rice, J.R. and Rosengren, G.F., 'Plane-strain deformation near a crack tip in a power law hardening material', J. of Mechs. and Phys. of Solids, 16, 1968, 1-12.

17. McClintock, F., 'Plasticity aspects of fracture', Fracture, Vol. III, Ed. Liebowitz, H., Academic Press, New York, 1971, pp, 47-225.

18. Broberg, K.B., 'Crack growth criteria and nonlinear fracture mechanics', J. Mechs. and Phys. of Solids, 19, 1971, pp. 407-418.

19. Rice, J.R. et al., 'Some further results of J integral analysis and estimates', in Progress in flow growth and fracture toughness testing, 1973, ASTM-STP 536, pp. 231-45.

20. Buzzard, R.J. and Fisher, D.M., 'Load-displacement and work deformation in three-point bend tests', J. of Testing and Evaluation, JTEVA, Vol. 6, No. 1, Jan. 1978, pp. 35-39.

21. Davis, M.G., 'Elastic-plastic fracture toughness based on the COD and J-contour integral concepts', Elastic-Plastic Fracture, ASTM STP 668.

22. Joyce, J.A. and Paris, P.C., 'Direct evaluation of J-resistance curves from load displacement records', Fracture Mechanics, ASTM STP 700, 1980, pp. 232-36.

23. Irwin, G.R. and Roland de Wit, 'A summary of fracture mechanics concepts', J. of Testing and Evaluation, JTEVA, Vol. 11, No. 1, Jan. 1983.

24. Clarks, G.A., Begley, J.A. et al., 'A procedure for the determination of ductile fracture toughness values using J integral techniques', J. of Testing and Evaluation, Vol. 7, No. 1, Jan. 1979.

25. Chipperfield, C.G., 'A summary and comparison of J estimation procedures', J. of Testing and Evaluation, Vol. 6, No. 4, July 1978.

26. Landes, J.D. and Begley, J.A., 'The effect of specimen geometry on J_{1c}', ASTM STP 514, 1972, pp. 24-39.

27. Rice, J.R., Bucci, R.J. and Landes, J.D., 'J integral estimation procedures', ASTM STP 514, 1972, pp. 40-69.

28. Landes, J.D., Begley, J.A. and Clarke, G.A., 'Elastic-plastic fracture', ASTM STP 668, 1977.

29. Landes, J.D. and Latzko, D.G.H., 'Post-yield fracture mechanics', Second Edition, 1984, Elsevier Applied Science Publishers, London and New York.

30. 'A general introduction to fracture mechanics', A Journal of Strain Analysis Monograph, Mechanical Engineering Publications Limited, London.

31. 'Developments in fracture mechanics test methods standardization', Editors, Brown W.F. and Kaufman, J.G., ASTM STP 632, 1976.

32. Kare Hellan, 'Introduction to fracture mechanics', 1984, McGraw-Hill Book Company.

33. 'Advances in elasto-plastic fracture mechanics', Ed. by Larsson, L.H., 1979, Applied Science Publishers Ltd., London.

34. Robinson, J.N., 'An experimental investigation of the effect of specimen type on the crack tip opening displacement and J integral fracture criteria', Int. J. of Fracture, Vol. 12, No. 5, Oct. 1976.